

Bucknell University

Bucknell Digital Commons

Master's Theses

Student Theses

Spring 2024

Energy Harvesting for Residential Microgrid Distributed Sensor Systems

Devin C. Whalen

Bucknell University, dcw020@bucknell.edu

Follow this and additional works at: https://digitalcommons.bucknell.edu/masters_theses



Part of the [Power and Energy Commons](#), and the [Systems and Communications Commons](#)

Recommended Citation

Whalen, Devin C., "Energy Harvesting for Residential Microgrid Distributed Sensor Systems" (2024).
Master's Theses. 278.

https://digitalcommons.bucknell.edu/masters_theses/278

This Masters Thesis is brought to you for free and open access by the Student Theses at Bucknell Digital Commons. It has been accepted for inclusion in Master's Theses by an authorized administrator of Bucknell Digital Commons. For more information, please contact dcadmin@bucknell.edu.


Energy Harvesting for Residential Microgrid Distributed Sensor Systems

By

Devin Connor Whalen

(A Thesis)

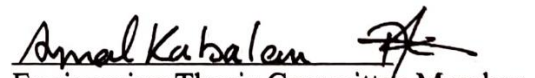
Presented to the Faculty of
Bucknell University
In Partial Fulfillment of the Requirements for the Degree of
Master of Science in Electrical Engineering

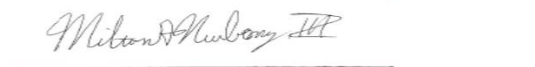
Approved: 
Adviser


Department Chairperson


Engineering Thesis Committee Member


Engineering Thesis Committee Member


Engineering Thesis Committee Member


Engineering Thesis Committee Member

April 2024

(Date: Month and Year)

Abstract

Microgrids are localized, independent power grids that can operate while connected to the larger electrical grid. These systems make intelligent decisions regarding power management and use an array of components to monitor power generation, consumption, and environmental conditions. While this technology can save end users money, the complexity of installation and maintenance has limited the adoption of microgrids in residential spaces. To simplify this technology for end users, the next evolution of microgrid components includes sensors that are wireless and ambiently powered.

Even with a microgrid installed, significant energy is wasted in residential spaces. To address this loss, energy harvesting circuits can be incorporated into microgrid sensors, enabling them to recapture otherwise wasted environmental energy. Light, heat, radio frequency (RF) energy, mechanical energy, and 60 Hz noise from power lines are all abundant in most residential spaces and can be harvested to power microgrid components. Equipping microgrid sensors with energy harvesters simplifies the end user experience by eliminating the need for cable routing. Implementing energy harvesting techniques results in a microgrid that is easier to deploy, cleaner, and requires less maintenance.

Developing this type of sensor is not only feasible, but sensible and can be constructed using off-the-shelf components. My research led me to conclude that the most effective strategy for designing an energy harvesting sensor is to combine energy harvesting technologies with battery power. By delegating smaller loads away from the harvesting integrated circuit (IC), its full harvesting potential is utilized, maximizing

energy collection for the power-hungry transmitter. Simultaneously, a small coin-cell battery can sustain the remaining components, ensuring over a decade of functionality. This thesis explores the feasibility and design of a hybrid battery and energy harvesting sensor. The developed system block diagram allows for the swapping of components within each block, catering to the varying needs of the end user. The system is data and energy-aware, allowing it to make intelligent decisions regarding data transmission and enable communication as reliable as that of a traditional wire-line powered sensor.

The hybrid sensor module underwent testing with a small monocrystalline solar cell as its energy source, delivering consistent power throughout the testing period. It accumulated surplus energy in a super capacitor storage unit, ensuring the system's reliable operation even at night when the energy source was not available. While the tests utilized a photovoltaic (PV) cell, the design accommodates any energy harvesting source that can generate a minimum of $40 \mu\text{W}$ of power.

Acknowledgments

I would first like to express my gratitude to my thesis adviser, Professor Peter Mark Jansson, for his unwavering support and confidence in my abilities. Our discussions constantly challenged me to advance my project, my research, and myself, pushing me to grow as an engineer and as a person.

I would like to express my sincere gratitude to the members of my thesis committee, Professors Stewart Thomas, Amal Kabalan, Richard Kozick, and Dr. Milton G. Newberry. I am grateful for the time that they all took to review my work, attend committee meetings, and provide feedback from each of their unique perspectives. I would like to extend a special thanks to Professor Stewart Thomas for inspiring my chosen topic, consistently making time for meetings beyond class hours, and dedicating extra effort to help publish my results.

Next, I would like to thank Matt Lamparter for his support of my project. Matt has played a pivotal role during both my undergraduate and graduate education. Thank you for always making time to explore ideas with me, assisting me in solving problems, and for your patience while I learned to use equipment.

I would like to thank Bucknell University's Department of Electrical and Computer Engineering and all the professors that have helped shape my educational journey. I would like to thank Professor Alan Cheville for first introducing me to Bucknell's graduate program and encouraging my pursuit of a Master of Science since my first campus visit. I would also like to thank the individuals I interviewed, Ben Levine, Hartin Code, John Kelchner, and Nate Johnson. Your valuable insights helped shape the direction of my project.

Finally, I would like to thank my friends and family, especially my parents, Jennifer and Richard Whalen. Thank you for your steadfast encouragement of my interests in engineering and pursuit of higher education. Your support, guidance, understanding, and love have shaped me into the person I am today, and I would not be here without you.

Table of Contents

Abstract	ii
Acknowledgments	iv
List of Tables	ix
List of Figures.....	x
Chapter 1: Introduction	12
1.1 Microgrid	12
1.2 Energy Harvesting	14
1.3 Thesis Questions	15
Chapter 2: Background	15
2.1 Situation Analysis	15
2.2 Literature Review	17
2.2.1 The Value of Microgrid	17
2.2.2 Sensors in Microgrid	20
2.2.3 Energy Harvesting	21
2.2.3.1 Radio Frequency (RF) Harvesting:	25
2.2.3.2 Power Line Scavenging	27
2.2.3.3 Photovoltaic (PV) Harvesting	28
2.2.3.4 Thermoelectric Harvesting	30
2.2.3.5 Piezoelectric Harvesting	30
2.2.3.6 Takeaways	32
2.3 Money and Energy Savings Study	33
2.4 Interviews	35

Chapter 3: Harvesting Source Evaluation	38
3.1 RF	38
3.2 Piezoelectric	42
3.3 Heat	44
3.4 Light	47
3.5 Source Comparison	52
Chapter 4: Harvester Design	55
4.1 Feasibility Study	55
4.1.1 Proving the Initial Hypothesis	55
4.1.2 Excess Energy Reservoir	60
4.1.3 Long Term Storage: Battery vs. Supercapacitor	61
4.2 Prototype Design	64
4.2.1 Harvester Choices	66
4.2.2 LTC3108 Analysis	66
4.3 Low Power Microcontrollers	68
4.3.1 Microcontroller Choices	68
4.3.2 MSP430G2553 Analysis	69
4.4 Sensors for Microgrid IoT	71
4.4.1 Chosen Sensors	72
4.4.2 Temperature and Occupancy Sensor Analysis	73
4.5 RF Transmitter	73
4.5.1 Communication Protocol	74
4.5.2 Some Transmitter Options	76

4.5.3	Xbee S1 Analysis	77
4.6	System Power Budget	79
4.6.1	Excess Energy Reservoir	83
Chapter 5: Data Collection and System Analysis		84
5.1	Experiment 1	84
5.2	Experiment 2	86
5.3	Experiment 3	93
Chapter 6: Conclusion		96
6.1	Contributions to Knowledge	97
6.1.1	Assessing the Viability of Powering a Microgrid Sensor with Energy Harvesting	97
6.2	Lessons Learned	99
6.2.1	Timing	99
6.2.2	UART Pulling Current	100
6.2.3	Sensor Accuracy	101
Chapter 7: Next Steps		102
7.1	Cost Analysis	102
7.2	Integration With Residential Microgrid	103
7.3	Energy Harvesting Standard	104
7.3.1	Challenges in Component Selection:	104
7.3.2	Towards a Standardized Framework:	105
Appendix 1. MSP430G2553 Code		107
References		112

List of Tables

Table 1: Harvesting Source Power Density (Data From “Energy Harvesting Techniques for Monitoring Devices in Smart Grid Application” [30])	24
Table 2: Harvesting Source Power Density (Data From “Ambient RF Energy-Harvesting Technologies for Self-Sustainable Standalone Wireless Sensor Platforms” [31])	25
Table 3: Power Draw of LEDs and Devices Typically Left on During Absence or at Night	34
Table 4: Number of People That Traveled Through a Single Entrance in the ELC	43
Table 5: Temperature of Common Devices	44
Table 6: Effect of Capacitor Size on RF Transmitter	56
Table 7: Commonly Used Energy Harvesting ICs	66
Table 8: Commonly Used Low-Power Microcontrollers	68
Table 9 Wireless Communication Technologies Compared [7]	74
Table 10: Explored Transmitter Options	76
Table 11: Daily Energy Consumption of System Components	82
Table 12: Component Prices	103

List of Figures

Fig. 1. Residential microgrid architecture.....	13
Fig. 2. 2.4GHz power sweep for the AD8318 logarithmic amplifier	40
Fig. 3. Power producible by a single Peltier TEG	47
Fig. 4. IV curve in direct sunlight.....	49
Fig. 5. IV curve for south-facing window.....	50
Fig. 6. IV curve for north-facing window.....	51
Fig. 7. IV curve in different lighting conditions	51
Fig. 8. Ambient energy sources compared on a logarithmic scale	53
Fig. 9. Expected capacitor voltage behavior for feasibility study.....	58
Fig. 10. Proposed capacitor voltage behavior for energy-aware system	59
Fig. 11. Hybrid battery and energy harvesting system block diagram	64
Fig. 12. Measured efficiency curves for power management boost converter	67
Fig. 13. MCU time between cycles (left) and active cycle time (right).....	79
Fig. 14. Predicted lifespan for 1 Ah battery	82
Fig. 15. System energy budget.....	83
Fig. 16. Collected temperature data between 12:00 PM and 5:00 PM March 5.....	85
Fig. 17. Hybrid energy harvesting sensor experimental setup.....	86
Fig. 18. Temperature data collected between March 6 and March 10 with a 1.5 F excess energy reservoir	87
Fig. 19. Gap in transmission due to energy shortage.....	88

Fig. 20. Temperature data collected between March 10 and March 18 with a 3 F excess energy reservoir	89
Fig. 21. Gap in transmission due to energy shortage	90
Fig. 22. Temperature data collected between March 19 and March 22 with a 4.5 F excess energy reservoir	91
Fig. 23. Temperature data and glitched transmissions.....	92
Fig. 24. Temperature data collected between March 29 and April 2 with data-aware program and a 4.5 F excess energy reservoir.....	93
Fig. 25. Temperature data collected on March 31	94
Fig. 26. Occupancy data collected between March 29 and April 2 with PIR interrupts ...	95
Fig. 27. Temperature data collected with data-aware approach and 3 F excess energy reservoir	96

Chapter 1: Introduction

1.1 Microgrid

Since the electrical grid was created, the supply of electricity has been required to meet the demand of the load connected to it. Not every device is connected to the grid at the same time, but the electricity supply is always available to accommodate periods of peak load throughout the day. Electricity not used during off-peak hours is wasted. Though excess energy can be stored in batteries, it is more efficient to use it immediately. Microgrid technology shifts the paradigm of an energy supply that must match the demand, to that of an energy demand that attempts to match the supply [1], [2]. Rather than expecting the grid to keep up with increasingly high peak loads, it makes more sense to match demand with the amount of power available whenever possible.

On a residential scale, a home controller connected to smart plugs can regulate the status of various power-hungry devices [3]. In residential spaces, there are devices which must remain on to maintain the comfort of the resident. These include HVAC and lighting for example. There are also “discretionary” devices, which can be powered on and off intermittently throughout a day without greatly affecting the home environment. Dish washers, clothing washers and dryers, refrigerators, and electric vehicles fall into this category. By making some predictions about the availability and price of electricity, a home controller can create an “optimum load shape” that governs which devices should be on at different times to use the energy available most effectively [4]. These predictions can be based on the day-ahead and real-time energy market, as well as the time of use (TOU) tariffs, which attempt to incentivize individuals to use more power during off-

peak hours. An automatic load management system can drastically reduce peak loads and save money by using electricity when it is cheaper [5], [6], [7].

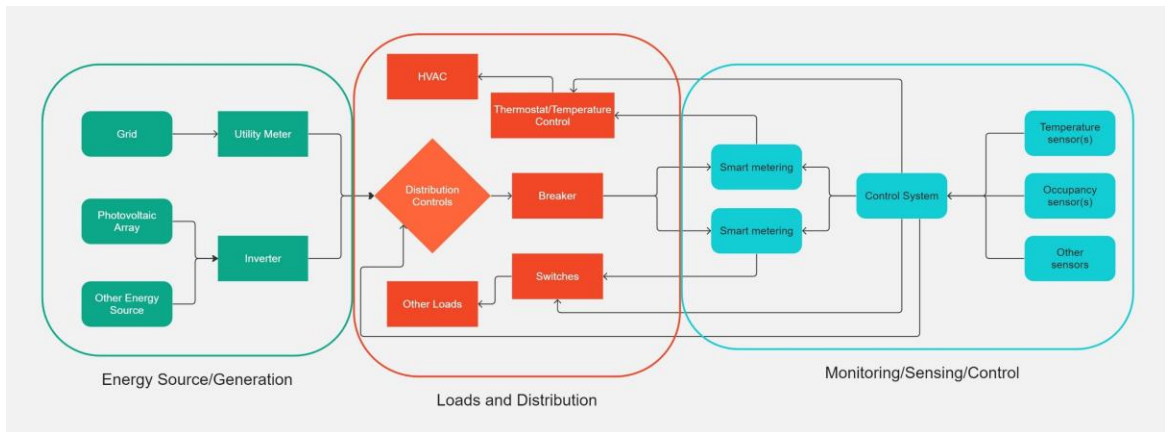


Fig. 1. Residential microgrid architecture

The concept of microgrid encompasses the evolution of the power grid into a next-generation system, featuring enhanced power management through the integration of advanced communication technologies and capabilities for increased control and efficiency [3]. While the terms “microgrid” and “smart grid” (used interchangeably) cover various domains, the aspect of energy management in residential spaces remains relatively under-adopted [3]. Fig. 1 shows the basic flow of a smart grid system. The primary objective of my research is the implementation and proof-of-concept of using energy harvesting to power microgrid components. Specifically, the project investigates the effectiveness of energy harvesting technologies within residential microgrid systems in reducing labor for the end user. The goal is to show that components that leverage energy harvesting are easier and quicker to install, thus encouraging the adoption of residential microgrids.

Although I believe that many devices within the monitoring, sensing, and control section of a residential microgrid could be powered with energy harvesting, my research focuses on sensing because these devices add the most value to the system and benefit the most from energy harvesting [8]. With the implementation of microgrid technology into home energy management systems [HEMs], the energy supply paradigm shifts from one that must match instantaneous demand to one that can now attempt to match to the supply. It is more practical to match the demand with the available power rather than to expect the grid to keep up with increasingly high peak loads [1].

1.2 Energy Harvesting

Energy harvesting refers to the method by which electrical energy is captured from surrounding environmental sources and then stored. Typically, solar, thermal, mechanical, and wind energies are the primary ambient energy sources used in energy harvesting processes [9]. A major advantage of energy harvesting is the ability to power a network of devices without drawing additional power from the grid. This approach not only reduces the energy consumption of the system but also enables easier, faster deployment and installation in hard-to-reach spaces, as it eliminates the need for wires.

Energy harvesting components also mitigate reliance on battery storage technology. The harvested energy can either be consumed immediately or stored in a supercapacitor until the required amount has been collected. Supercapacitors do not need frequent maintenance or replacement after long periods, unlike traditional batteries, significantly reducing the total cost of ownership and maintenance necessary for the microgrid system. However, batteries have much higher specific energy capacity compared to supercapacitors, making them more appropriate where longer-term storage

is necessary. While the optimal energy storage method may differ based on the application, my results show that a system powered with a supercapacitor can operate as robustly as a system equipped with a lithium-ion battery.

1.3 Thesis Questions

The exploration of energy harvesting within residential microgrid systems is guided by several questions that form the foundation of this thesis. These inquiries explore the potential and viability of ambient energy sources and seek to determine the practicality of powering microgrid sensors exclusively through harvested energy. The main questions I aim to answer are as follows:

- 1) What types of ambient energy sources are available in residential spaces and which provide the highest energy density?**
- 2) Is it possible to reliably power a microgrid sensor using energy harvesting?**

By addressing these questions, my research reveals the feasibility and efficiency of integrating energy harvesting technologies into home energy management systems. This investigation is crucial for advancing our understanding of sustainable energy solutions and their role in reducing dependency on the traditional power grid.

Chapter 2: Background

2.1 Situation Analysis

As the global population continues to grow, so does the planet's energy needs. Current population estimates of 8.1 billion people are projected to surpass 9 billion by

2050, driven by increasing global industrial development [10], [11]. This growth is closely linked to the demand for energy, which varies with a country's infrastructure and industrialization [10]. Notably, global household consumption, constituting nearly 30% of total energy consumption, aligns with the pace of gross domestic product (GDP) growth [11]. According to another study, public energy consumption represents about 30% of the global consumption in western countries, and home consumption represents about 18%, a sufficiently large percentage to warrant the application of new technologies for more efficient control and management of this energy [3]. According to the 2023 Annual Energy Outlook report of the U.S. Energy Information Administration, residential electricity consumption is projected to increase between 14% and 22% by 2050 [5], [12], [13].

The primary objective of the traditional grid is to serve customers through a unidirectional system, consisting of four key components: production, transmission, distribution, and consumption [14]. Substantial residential energy consumption and its capacity for demand response [15], [16] have prompted the U.S. government to significantly stress the importance and need for demand response efforts among residential customers [17], [4]. In the U.S., the average age of power-grid transmission lines is above 50–60 years [8], [18]. To avoid blackouts and power disruptions, and to guarantee reliability and efficiency, it is essential to update the grid by modernizing and incorporating smart technology [14]. Addressing the challenges posed by aging infrastructure, population growth, and escalating energy needs, residential microgrids emerge as a viable solution.

Microgrids aim to enhance the efficiency, reliability, safety, sustainability, and flexibility of electrical energy systems, encompassing generation, transmission, distribution, and end-use consumption. Moreover, the smart grid seeks to integrate renewable energies into these systems [19]. This transformation could bolster global energy security, support the continuation of economic growth, and address environmental issues, including climate change. As the pursuit of greener, more efficient solutions persists, the demand for energy harvesting technologies increases [13].

2.2 Literature Review

2.2.1 The Value of Microgrid

The initial inquiry to address is the rationale behind microgrids and existing research surrounding them. Numerous studies highlight the benefits of microgrids, with a significant focus on the advantages of large-scale or commercial implementations. Due to the difficulties, time, and costs involved in securing cooperation from individual end users, the trend has shifted towards utility-level microgrids rather than those at the residential level. Yet, with the continuous rise in residential demand, the capability of utility-scale microgrids to regulate electrical loads is becoming increasingly constrained. Furthermore, the value proposition for end users is increasing. According to S. Damodaran and B. Sridharan, “The prime task of the smart grid is to manage the power demand and the power supplied during the peak conditions at least possible cost.” [6] The study explores the development of a systemwide framework to coordinate demand response of residential customers in a smart grid.

P. Diefenderfer, P. M. Jansson, and E. R. Prescott delve into the advantages of real-time sensing and monitoring of power characteristics, and how this data, when fed into control systems designed to optimize the grid, improves efficiency. They highlight the system's capability to track energy flow, utilize cloud communications, and leverage embedded sensors to manage energy costs and make forecasts, ensuring renewable energy is used in the most cost-effective manner. They propose that "Such an integrated and predictive system can also store thermal energy inaugurating a paradigm shift from a 'demand response market' to one that becomes an 'availability responsive market.'" [1]

In a similar vein, Amir Safdarian, Mahmud Fotuhi-Firuzabad, and Matti Lehtonen explore the "demand response coordination problem," highlighting the strategic coordination necessary to address it [4].

S. Nunez, M. Kabalan, P. Singh, and V. Moncada evaluate a prospective microgrid system for the La Kasquita Community in Nicaragua. Their evaluation includes an overview of the community's economic activities, educational background, and potential electricity usage per household. The paper also highlights community interest in such projects and reviews similar initiatives in the region. Additionally, it conducts an analysis of the community's hydro, wind, and solar energy potential relative to its energy needs. The conclusion of the paper proposes a model designed to fulfill the community's energy requirements [20]. In another study, these authors emphasize the importance of proper design, construction, and operation of microgrids, underscoring the need for knowledge and expertise in electrical engineering. The paper shares insights gained from the commissioning of an industry-grade microgrid, which was achieved with the involvement of undergraduate and graduate students [2].

Hanaa Talei et Al. explore campus-wide microgrid systems, compiling data from seven different university microgrids. The Illinois Institute of Technology Microgrid entitled “Perfect Power” aimed to create a microgrid model that could be used throughout the country and reduce the peak demand at the university by at least 20% [14]. Meanwhile in 2011 when Japan experienced a magnitude 9 earthquake, the Sendai microgrid operating on Tohoku Fukushi University successfully supplied uninterrupted power to hospitals and nursing care facilities, which were in dire need of both electricity and thermal energy. Learning from this, Japan committed to developing a range of diversified energy source microgrids across the nation, aiming to maintain energy supply during disasters [14], [21]. These case studies all highlight the value proposition of microgrid technology. “The electrical grid needs to be intelligent, reliable, and flexible in coping with the increased peak demand, to avoid brown outs and black outs, as well in integrating distributed energy resources such as solar and wind to avoid building big centralized generators.” [14]

While the aforementioned studies have focused on large-scale microgrid, Francisco J. Bellido Outeiriño et Al. explore the advantages of residential-scale in-home power management systems based on wireless sensor networks (WSN). While it is common to concentrate solely on achieving maximum energy savings through large-scale energy management systems, managing small devices across numerous households can yield significant benefits. Francisco J. Bellido Outeiriño captures this sentiment by stating, “Plugging in a device is so simple and routine that we’ve overlooked the energy cost it incurs, both economically and socially” [3]. The study delves into the development and assembly of a mains-powered sensor module aimed at home energy management,

capable of measuring the instantaneous power of residential loads, as well as temperature and light levels. Data collected by the module is transmitted to a distinct controller module via a ZigBee transmitter, which then oversees the management of residential Alternating Current (AC) loads.

M. Erol-Kantarci and H. T. Mouftah further underscore the importance of managing energy in residential settings. Their research focuses on the effectiveness of an in-home energy management (iHEM) application. It compares iHEM's performance against an optimization-based residential energy management (OREM) system, designed to lower energy costs for consumers. The findings demonstrate that iHEM not only cuts energy expenses but also diminishes the consumers' contribution to peak load, lowers the household's carbon emissions, and achieves savings nearly equivalent to those of OREM [5].

2.2.2 Sensors in Microgrid

The previous section established the value that microgrids offer. "Use of intelligent control and power management is one of the crucial points for the microgrid operation" [22]. At all levels, sensor nodes enable microgrid systems to make intelligent decisions. The next step is to establish the importance of and requirements for an effective microgrid sensor.

Masanobu Honda, Takayasu Sakurai, and Makoto Takamiya had the following to say regarding their 2015 study of a power line energy scavenging sensor. "In the building energy management system (BEMS), sensor nodes are required to monitor the indoor environment (e.g., temperature, humidity, and illuminance) and the measured data are

used to control the air conditioning and the lighting of the building for reducing the energy consumption. The requirements of the sensor nodes for BEMS are: (1) low cost installation, (2) low operational cost, and (3) stable and continuous monitoring” [23].

Vehbi C. Gungor, Bin Lu, and Gerhard P. Hancke highlight the significance of intelligent sensors in their study on the prospects and challenges faced by wireless sensor networks in the smart grid, stating, “Intelligent and low-cost monitoring and control enabled by online sensing technologies have become essential to maintain safety, reliability, efficiency, and uptime of the smart grid [8].” Similarly, Shivangi Verma and Poonam Rana emphasize the need for effective sensing and communication within microgrids, noting, “Smart grid environments require high standard of consistent communication technologies to support various types of electrical services and applications” [7]. The critical role of smart sensing technologies is further reinforced in references [24], [25], [26], [27].

Consequently, it is imperative to ensure that these technologies are designed for straightforward integration. “Due to various services provided by an EMS, the integration of the system into a microgrid will result on the exchange of huge amount of data to make important decision and ensure that the microgrid is operationally stable” [14].

2.2.3 Energy Harvesting

Implementing energy harvesting can help ease sensor integration and reduce system maintenance by eliminating the need for batteries, thus contributing to maximizing the effectiveness of microgrid systems. Energy harvesting technology is not a new concept. J. A. Paradiso and T. Starner highlight how the history of energy

harvesting traces back to the water wheel and windmill, with viable methods for capturing energy from waste heat or vibration existing for several decades. “Exploiting renewable energy resources in the device’s environment...offers a power source limited by the device’s physical survival rather than an adjunct energy store.” [28]

Batteries are the main power source for most low-power remote sensor devices and embedded systems. However, batteries have limited lifetimes and need to be replaced periodically. This replacement cycle introduces challenges, not just in terms of cost and maintenance but also regarding environmental impact due to battery waste.

By integrating energy harvesting technologies into electronic devices, they can operate independent of human intervention. As L.-G. Tran, H.-K. Cha, and W.-T. Park note, “By applying power harvesting technologies, devices and equipment can become self-sustaining with respect to the energy required for operation, thereby obtaining an unlimited operating lifespan. Thus, the demand for power maintenance will become negligible.” [29]

This sentiment is echoed by H Pavana and Rohini Deshpande in their observation that one of the primary limitations of wireless sensor nodes is the finite lifetime of batteries, which deplete over time. “Energy harvesting techniques can be used to overcome this constraint and has the ability to make wireless sensor node self-sustainable” [30].

The shift away from batteries not only addresses the issue of their limited lifetimes but also aligns with environmental sustainability goals. Implementing energy harvesting technology diminishes reliance on batteries, which in turn reduces battery waste, which then lessens environmental damage. Furthermore, the method of capturing

environmental energy for power is a clean source that does not produce waste. “The most effective solution for reducing battery waste is to avoid using them. Applying Wireless Power Harvesting (WPH) technology will help to reduce the dependency on batteries, which will ultimately have a positive impact on the environment. Moreover, the process of harnessing electromagnetic energy will not generate waste, as it is a clean energy source” [29].

The miniaturization of electronics and their reduced power needs have fueled the explosion in wireless and mobile applications we see today. While cost-effective batteries have been pivotal in this growth, they also represent a bottleneck. The ambition for ubiquitous computing with wireless sensors is curtailed by the logistical and environmental issues associated with battery replacement and disposal. “As electronics became smaller and required less power, batteries could grow smaller, enabling today’s wireless and mobile applications explosion. Although economical batteries are a prime agent behind this expansion, they also limit its penetration; ubiquitous computing’s dream of wireless sensors everywhere is accompanied by the nightmare of battery replacement and disposal” [28].

The transition towards energy harvesting technologies represents a crucial shift in how we operate low-power devices, offering a sustainable path forward that could minimize maintenance demands, reduce environmental harms, and ultimately enable the broader adoption of wireless and mobile technologies. H Pavana and Rohini Deshpande explore the power densities of different harvesting sources [30] in Table 1:

Table 1: Harvesting Source Power Density (Data From “Energy Harvesting Techniques for Monitoring Devices in Smart Grid Application” [30])

Energy Sources	Power Density mW/cm ²
Solar	20
Wind	1
Vibration	0.33
Magnetic Field	0.282
Electric Field	0.17
Thermal	0.05
RF	0.001

Sangkil Kim et Al. present similar information, summarizing widely used ambient energy sources and their respective pros and cons. Table 2 shows their findings [31]. The study offers additional proof of the significantly higher energy density that solar energy delivers while also presenting thermal, RF, and piezoelectric harvesting as promising options.

Table 2: Harvesting Source Power Density (Data From “Ambient RF Energy-Harvesting Technologies for Self-Sustainable Standalone Wireless Sensor Platforms” [31])

	Solar Energy	Thermal Energy	Ambient RF Energy	Piezoelectric Energy	
				Vibration	Push Button
Power Density	100 mW/cm ²	60 μW/cm ²	0.0002 ~ 1 μW/cm ²	200 μW/cm ³	50 μJ/N
Output	0.5 V (single Si cell) 1 V (single a-Si cell)	-	3 – 4 V (open circuit)	10 – 25 V	100 – 10000V
Available Time	Day Time (4 ~ 8 Hrs)	Continuous	Continuous	Activity Dependent	Activity Dependent
Weight	5 ~ 10 g	10 ~ 20 g	2 ~ 3 g	2 ~ 10 g	1 ~ 2 g
Pros	- Large amount of energy - Well-developed tech	- Always available	- Antenna can be integrated onto frame - Widely available	- Well-developed tech - Light weight	- Well-developed tech - Light weight - Small volume
Cons	- Needs large area - Non-continuous - Orientation issue	- Needs large area - Low power - Rigid and brittle	- Distance Dependent - Dependent on available power source	- Needs large area - Highly variable output	- Highly variable output - Low conversion efficiency

Similar comparisons are explored by Fernando Moreno Cruz et. Al in in their study “Why Use RF Energy Harvesting in Smart Grids?” [19] and Kok Tung Thong et Al. in “Data Acquisition System for Piezoelectric Cymbal Transducer Energy Harvesting” [32]. Although the exact power densities vary slightly, the hierarchy of energy harvesting sources is consistent. The subsequent sections explore the studies conducted on the prevalent types of energy harvesting in more detail.

2.2.3.1 Radio Frequency (RF) Harvesting:

Passive Radio Frequency Identification (RFID) tags capture electrical energy from the incoming RF signal to transmit data. However, the technical challenges related

to RF energy harvesting are distinct from those in RFID systems. In RFID technology, an intense radio emission from a reader prompts a tag to respond using a backscattered radio signal [33]. The tag remains inactive until it is activated by the reader's scan. Unlike RFID systems, where data transmission relies on reader activation, wireless sensor nodes must proactively collect and transmit data. "Moreover, since the amount of power harvested from ambient RF fields is limited, wireless sensor nodes need to operate intermittently" [33].

J. Zhang et Al. present a rectenna (rectifying antenna) design that is optimized for wideband high-gain RF energy collection. This design features a double-sided antenna, accompanied by a low-pass filter and a rectifying circuit that employs Schottky diodes for the rectification process. The device is operational across a frequency spectrum from 1.9 to 3.2 GHz. Simulation data shows that this rectenna achieves a peak conversion efficiency of approximately 70% at 2.4 GHz, given an incoming power density of $50 \mu\text{W}/\text{cm}^2$ and could therefore harvest ambient RF energy in the air. Across its entire operating frequency range, the device maintains a conversion efficiency exceeding 50% [34]. Hakim Takhedmit explores a similar rectenna circuit, designed to use the Industrial Scientific and Medical (ISM) band at 2.45 GHz to wirelessly power a batteryless temperature sensor. Experimental results showed that the circuit achieves over 80% efficiency at both medium and low power densities. This circuit features a symmetric, dual-access RF-to-DC rectifier and two patch antennas. The temperature sensor conducted readings every 10 seconds, requiring a voltage of 1 V and $30 \mu\text{J}$ of energy for each measurement cycle. It was capable of operating with power densities as little as $0.4 \mu\text{W}/\text{cm}^2$ ($E = 1.22 \text{ V}/\text{m}$) [35].

Hiroshi Nishimoto, Yoshihiro Kawahara, and Tohru Asami propose the use of RF noise to power sensor nodes. “Energy harvesting is a key technique that can be used to overcome the barriers that prevent the real world deployment of wireless sensor networks (WSNs). [33] The paper proposes RF harvesting as an alternative to solar energy harvesting to mitigate reliance on battery technology. Unlike solar energy, RF noise is often available at night. While it is regularly available, the amount of harvestable power is a fraction of solar.

L.-G. Tran, H.-K. Cha, and W.-T. Park offer an overview of RF power harvesting technologies, aiming to inform the design of RF energy harvesting units. Given that these circuits operate with relatively low voltages and currents, they depend on cutting-edge electrical technology to achieve high efficiency. The authors analyze and discuss different designs along with their compromises. Additionally, they outline recent applications of RF power harvesting [29].

2.2.3.2 Power Line Scavenging

Another method of energy harvesting involves capturing the alternating magnetic fields produced by AC power lines, utilizing magnetic energy harvesting cores. In their research, M. Honda, T. Sakurai, and M. Takamiya investigate the harvesting of energy from AC power lines. Their system employs two copper diodes positioned along an AC power cable to harvest energy. This collected AC energy is then converted into Direct Current (DC) through a basic bridge rectifier and stored in a capacitor. A voltage detector keeps track of the capacitor’s charge and initiates transmission whenever energy is available. The system continuously transmits as long as there is enough collected energy, without specifically being energy or data-aware [23].

Joseph Cheang et Al. investigate another method of non-intrusive powerline energy scavenging to operate an MCU and AC power meter. The study proposes applications in residential wireless AC line metering. The authors suggest that excess energy be stored in a backup battery or supercapacitor hybrid. The system is intended for use with wireless sensors in AC power monitoring applications. “Current transformer coupling with the power line facilitates simple ‘snap-on’ installation of the sensors without interruption of power to customers.” Though they present a compelling block diagram that includes intelligent sensing controlled by an MCU and an excess energy reservoir, the paper does not indicate that they built a prototype for their design or tested it in any real-world scenario [36].

2.2.3.3 Photovoltaic (PV) Harvesting

Previously discussed studies about the energy density of different harvesting sources each indicated that PV has the highest capacity. Although solar is widely available and rich in power density, H Pavana; Rohini Deshpande point out that the major drawback of solar transducers is that they are “time dependent and real time monitoring requires continuous flow of energy” [30]. Toshihiko Ishiyama also notes that “while ambient power generation using solar power is a strong candidate to consistently generate energy throughout the year, indoor lighting is said to be equal to only 1/100 – 1/1000 of the daytime outdoor sunlight brightness” [37]. Despite these observations, solar harvesting remains a compelling choice due to its high energy density, suggesting the potential to accumulate and store surplus energy for nighttime use.

Achim Berger et. Al explore applications of PV energy harvesting sensors in industrial applications. Their study explores the effectiveness of two different

commercially available energy harvesting ICs at harvesting from a PV cell in indoor lighting conditions [38]. They tested their harvesting circuit in simulated lighting conditions and then compared their results to the typical illuminance of an industrial environment. Although they conclude that their harvesting circuit suits industrial settings, it lacks data from real-world conditions.

Many of the studies discussed so far have targeted industrial or commercial applications of WSNs. Toshihiko Ishiyama explores applications of energy harvesting sensors in residential spaces: “Since the advent of HEMS (home energy management system) and BEMS (building energy management system), various electronic devices in homes and offices are required to be controlled via a network [39], [40]. Such devices can be controlled in a single location centrally or in individual areas, such as rooms. In either case, the terminals transmitting data must be connected via a network” [37]. The paper explores the potential PV generation from indoor solar cells facing the sun through a window. While the data presented is intriguing and the application of HEMs falls within my scope of interest, the study’s data collection utilized an artificial load instead of an actual sensor device. The research offers notable details, such as the correlation between the maximum power output of a PV cell and illuminance, as well as the relationship between the charging time of a storage capacitor and its capacitance, which are specific to their selected PV transducers. However, the absence of a proof-of-concept system or real-world data collection is evident. Although their findings suggest the feasibility of developing a reliable energy harvesting sensor node, they stop short of providing definitive evidence.

2.2.3.4 Thermoelectric Harvesting

Thermoelectric harvesting transforms the temperature difference between two points into electricity through the thermoelectric effect. One limitation, however, is the intermittent availability of a thermal energy source, with the harvested power typically in the microwatt range [30].

D. Vadhel, S. Modhavadiya, and J. Zala delve into the capabilities of thermoelectric generators (TEGs) utilizing peltier tiles, providing insights into the power that can be generated under various heat gradients [41]. Further exploration by E. Ouserigha and A. Benjamin focuses on the SP1848 thermoelectric generator Peltier tile, detailing a design using a Bismuth Telluride-based generator module. This system includes a thermoelectric converter, heat source, cooling mechanism, and a voltage enhancer, demonstrating that voltage and current outputs increase with the temperature differential, peaking at a 70 °C difference with a maximum output of 2.2 V [42].

Highlighting the significance of their research, Vadhel, Modhavadiya, and Zala note the dire need for electricity in rural and isolated areas, home to around 1.3 billion people globally, with a substantial portion in India. They argue that thermoelectric generators, particularly in sun-drenched and heat-abundant locations, could be a vital energy source [41]. Ouserigha and Benjamin's work with the SP1848 module reveals its potential to power portable devices with its enhanced voltage output, indicating a promising avenue for thermoelectric energy in off-grid and underserved regions [42].

2.2.3.5 Piezoelectric Harvesting

Piezoelectric harvesting, which converts mechanical stress into electrical energy, presents another promising avenue for energy generation, particularly in urban

environments. Adnan Mohamed Elhalwagy, Mahmoud Yousef M. Ghoneem, and Mohamed Elhadidi have investigated the potential of piezoelectric-enabled floor tiles to capture energy from human footsteps [13]. Their research highlights the application of this technology in high-foot-traffic areas such as buildings and public spaces.

A specific study conducted by P. Abadi, D. Darlis, and M. Suraatmadja focused on an arrangement of 20 disc-type piezoelectric transducers configured in series and parallel within a small tile. This design aimed to optimize energy harvested from the action of a single footstep [43]. The findings revealed that such a setup could generate an average of 60.4 milliwatts per 10 footsteps. The study utilized Lead Zirconate Titanate (PZT) piezoelectric transducers, demonstrating that a tile equipped with 20 of these transducers in parallel could produce an AC voltage as high as 71.20 V, with an average output voltage of 63.98 V, translating to an average power output of 0.0604 watts per 10 footsteps [43].

M. Krishnasamy and colleagues expanded on the discussion, noting the viability of vibration-based energy harvesting systems, especially those employing Micro-Electro-Mechanical Systems (MEMS), for generating power across a wide spectrum, from milliwatts to several kilowatts. They emphasized human walking as a significant source of mechanical energy, particularly in densely populated urban centers such as airports, bus and railway stations, markets, and educational institutions. The abundance of mechanical energy in these settings, coupled with high population densities, makes them ideal for piezoelectric energy harvesting [9].

These studies collectively underscore the potential of piezoelectric technology to harness the everyday mechanical energy of human movements, offering a sustainable and

efficient method for generating electricity in urban environments. Though their potential application in residential spaces is not widely explored.

2.2.3.6 Takeaways

The literature review not only lays the groundwork by providing necessary background information but also pinpoints areas where my research can contribute significantly. It first established the value of microgrids, next it highlights the crucial function of sensors within microgrid infrastructures, noting that enhancing the usability and longevity of sensors inherently strengthens the robustness and effectiveness of microgrid systems. The discussion then pivots to energy harvesting as a strategy to bolster sensor effectiveness and ease installation. This approach not only diminishes reliance on batteries—thereby lowering maintenance requirements—but also harnesses otherwise wasted energy. Furthermore, it delineates which sources of energy harvesting are deemed most viable and examines ongoing research aimed at leveraging these sources to power electronic devices.

The survey of existing literature reveals a gap in the exploration of energy harvesting within the context of residential microgrids or home energy management systems. Although there is theoretical discussion about its potential applications, actual design and real-world testing are sparse. This scarcity contrasts with the abundant research focused on energy harvesting for industrial or utility-scale applications. As residential energy demands escalate, the logic of managing these demands at the consumer level becomes increasingly compelling.

Questions such as the viability of different harvesting sources, the requirements for energy-harvesting sensors, and whether such a sensor needs to be energy-aware, set

the stage for this research. The literature outlines the characteristics of an ideal microgrid sensor, including affordability, ease of deployment, and the capacity for reliable, uninterrupted monitoring [23]. Tingwen Ruan and Zheng Jun Chew underscore the criticality of energy awareness, pointing out the perennial challenge of aligning the energy produced by harvesters with the fluctuating and sometimes limited demands of Wireless Sensor Networks (WSNs) [44]. Many reviewed systems exhibit some level of energy awareness, transmitting whenever energy is sufficient. However, transmitting without data awareness or accounting for the intermittent availability of energy sources is unsustainable. This fact is especially true for solar energy, which is only accessible during daylight, highlighting the necessity for a strategy that allows for the accumulation and storage of excess energy for use during non-daylight hours.

The literature underscores a notable oversight in the application of microgrids within residential settings, signaling an opportunity for meaningful research in this area. For microgrid sensor nodes to be feasible, they must be cost-effective to install, inexpensive to operate, and capable of stable, continuous monitoring.

2.3 Money and Energy Savings Study

To further demonstrate the advantages of home energy management, I calculated the potential savings in energy and money that could be achieved by connecting a PIR sensor to various electrical loads. I used an Adafruit M4 Express microcontroller (MCU) connected to a simple passive infrared (PIR) sensor to detect when people were present in a four-person apartment. Using a P3 International “Kill A Watt” power meter, I measured the power draw of various devices that typically got left on at night and when no one was present. Table 3 shows the results. Additionally, the apartment contained 18 LED light

bulbs, which each drew roughly 10 watts when left on. These were turned off at night but were often left on during the day when residents were away.

Table 3: Power Draw of LEDs and Devices Typically Left on During Absence or at Night

Device	Ambient Power Draw	Number of Devices
Box Fan	62 watts	2
PC	85 watts	3
Monitor	40 watts	5
Printer	12.8 watts	1
3D Printer	22.8 watts	1
Power Strip: TV, Game Consoles, Apple TV	150 watts	1
Power Strip: Electric Tea Kettle, Standing Desk	30 watts	1
Computer Speakers	8 watts	1
LED Light Bulb	10 watts	18

Overall, I measured 772.6 W of power draw from ambient devices and an additional 180 W from lightbulbs when left on. Throughout 4 days, on average, no one was active in the apartment for 11 hours a day, this includes when residents were absent and when they were asleep. It is worth noting that the cat living in the apartment may have triggered the occupancy sensor at some times when no humans were present.

Additionally, these data were collected in December when the temperature was below 5 °C and no one living in the apartment had regular classes. Regardless, these devices account for over 9 kWh of wasted energy. As of December 2022, when the study initially took place, the average price of electricity in Pennsylvania was ¢13.57/kWh. Powering off unused devices during inactive hours would have resulted in savings of \$447.68 over a 1-year period. I am confident that the savings would be even greater with more accurate occupancy data and access to regulate more power-hungry systems like HVAC.

Using occupancy data to optimize HVAC systems for energy savings is not a novel idea. Research by Hamed Heidarifar and Mahdi Shahbakhti investigates the energy savings achieved in a residential setting using a Google NEST Thermostat E. The study utilizes two Monnit wireless PIR motion detection sensors placed on the first and second floors to monitor occupancy patterns. The thermostat adjusts the building's temperature by controlling a gas furnace, reducing heat when occupants are absent and prioritizing energy savings over comfort when possible. Their findings indicate that leveraging occupancy data can lead to a reduction in the building's energy consumption by up to 18.2% [45].

2.4 Interviews

Before beginning my own research, I interviewed several people in the power management and microgrid industry to get their insights about the important challenges faced by the industry and their feedback about my proposed topic.

Ben Levine is a project engineer with ME Engineers, a company that specializes in installing mechanical, electrical, plumbing, and technology (MEPT) systems in large-scale commercial developments, convention centers, higher education buildings, and

healthcare facilities. In our interview, he highlighted the intricacies of sensor network commissioning within large-scale structures. Levine’s observation, “The hard part about this that never gets done is the commissioning... hundreds of thousands of sensor values throughout – ensuring that that all those sensors are tied in and properly designated [is a challenge] – all you need to do to screw it up is mix up a room number” [46], underscores the potential benefits of a system designed to streamline sensor deployment and installation.

Hartin Code works for a company called Brainbox AI. The company targets large-scale commercial buildings and uses AI to perform predictive heating analysis. “Every 5 minutes, we pull data from every room in the building – feed it to the AI and predict the temperature of the room from 5 minutes to an hour” [47]. This approach underscores the adaptability of data transmission frequencies, even in data-intensive applications. Code also provided insight into why residential microgrids remain underexplored. “The number of buildings for commercial real estate that are under 100 square feet is higher, but the [total] number of square feet taken up by larger buildings is much greater. Targeting large scale buildings is going to save so much more energy than [targeting] many small ones” [47]. From a company perspective, the focus on large buildings for energy savings overshadows the smaller residential scale.

I also had the opportunity to interview John Kelchner and Nate Johnson, the former and current CEO of Citizen’s Electric, an electric utility company in Lewisburg, PA. According to Kelchner, Citizen’s Electric has “a pretty extensive network of meters that are remotely accessed [and] collect data on an hourly basis. [They are] far from real time. [It is] slow to communicate with them, [and they] can’t really bring back [data] in

an actionable time frame” [48]. Their system uses powerline communication for transmission, which is cheap, but slow. Kelchner’s observations highlight the opportunity provided by more immediate, local sensor-based load management.

Johnson emphasized the need for user-friendly solutions to encourage residential energy management adoption, noting, “From a regulatory perspective, [residents] are hesitant to take on this energy management. [We] don’t want to make it too hard for the average consumer” [49]. When asked to elaborate, Johnson added “[Complexity of installation] definitely contributes to the slow-moving machine. Power was built over a century [ago]. Stuff is operating the same way it was 100 years ago. Change makes people uncomfortable. Finding ways to more easily integrate new tech with old school infrastructure [could] reduce barriers to entry.” [49].

In discussing the most logical targets for regulation, Johnson highlighted electric vehicles (EVs). He noted, “As EV adoption increases, we’re likely to see greater integration into residential settings. By linking with homeowners’ EV chargers, we can provide more attractive pricing” [49]. The conversation also turned to other manageable loads, such as household appliances. Johnson mentioned, “There’s no need for me to be physically present to operate devices. For instance, my dryer is synced with a home energy management app, allowing me to schedule drying so my clothes are ready when I return home” [49]. This discussion on discretionary load management reflects a broader strategy for enhancing home energy efficiency. Additionally, when I previously consulted Ben Levine about primary energy consumers, he identified industrial lighting and HVAC systems as the top culprits [46].

These interviews underline the reasons behind the limited exploration of residential microgrid and load management systems: high investment costs, complex installations, and perceived low returns. However, they also highlight the growing need and potential for home energy management systems as energy demands rise. For such a transition to be successful, sensor technology must be affordable, low-maintenance, and easy to deploy. The discussions suggest focusing on regulating energy-intensive systems like HVAC and lighting, as well as discretionary loads, including home appliances and electric vehicles, providing a clear starting point for exploring effective load management strategies.

Chapter 3: Harvesting Source Evaluation

Although the preceding section delved into the current body of research on different forms of energy harvesting and their energy densities, I aimed to undertake my own investigations and experiments. This approach facilitates a more knowledgeable analysis of the most viable harvesting sources.

3.1 RF

Energy harvesting offers a solution to the obstacles preventing the widespread implementation of WSNs. Employing RF as an alternative energy source presents a viable option for powering wireless sensor nodes and addresses the challenges associated with intermittently available harvesting sources [33]. Though invisible, there are many RF signals surrounding the space in which people live and work. Signals like Wi-Fi,

cellular, radio, and TV are all forms of RF. Using an antenna to filter out a specific frequency, RF can be captured as a sinusoidal voltage. Using a rectifier circuit, this periodic voltage can be converted to a small amount of DC power [50].

Received power from RF is modeled by the Friis equation (1), where P_R is received power, L is the path loss factor, G_T is the gain of the transmitting antenna, G_R is the gain of the receiving antenna, λ is the wavelength, and d is the distance between the two antennas [51].

$$P_R = P_T \frac{G_T G_R \lambda^2}{(4\pi d)^2 L} \quad (1)$$

Modeling the amount of power received using this equation is good for designing systems where a large amount of RF is intentionally broadcasted for harvesting, but in this study, I am more interested in the amount of ambient RF present within different residential environments. Rather than modeling the potential power producible with the Friis equation, I measured the real amount of RF present in different spaces.

To capture the following data, I used a monopole whip antenna designed for the measured frequency in tandem with an AD8318 logarithmic amplifier module. The logarithmic amplifier converts the sinusoidal voltage captured by a frequency-specific antenna to a DC voltage that represents the amount of RF power present. The unit for this measurement is decibels relative to one milliwatt (dBm), which is the standard unit used to measure RF power and signal strength. To verify the relationship between the produced DC voltage and dBm, I used a benchtop RF power supply to artificially produce a range of power levels in the 2.4GHz band and plotted the response of the logarithmic amplifier for each.

According to one study, a Wi-Fi router can produce up to 20 dBm. If this router transmits an RF burst at 100 mW at 2.4GHz, then an object one meter away will receive only 10 μ W [29]. While some Wi-Fi routers may be capable of transmitting this much power, in testing, the measured power received is much lower. It is important to note as well that modern Wi-Fi routers limit the amount of broadcasted RF when connected devices are performing light tasks. RF measurements in my own apartment were taken with two devices streaming 4K video and a third downloading a large file. There was very little difference between measurements with and without the network load introduced, only resulting in a roughly 3 dBm difference. The insignificance of this difference may be due to the router used or insufficient strain on the system.



Fig. 2. 2.4GHz power sweep for the AD8318 logarithmic amplifier

In the Bucknell student space at a time full of students, the logarithmic amplifier produced 1.811 V, which corresponds to a measured power of -60 dBm or 0.9 nW. In an apartment within one meter of a standard Wi-Fi router, the log amp produced 1.43 V, corresponding to a measured power of -40 dBm or 0.1 μ W. In the Dana 303 classroom, the log amp produced as low as 0.998 V, corresponding to a measured power of -25 dBm or 3.16 μ W, although it is worth noting that this classroom sits directly below the school radio station. While it is not expected that these frequencies would interfere, elevated levels of RF were detected in this room.

The amount of power harvestable from ambient RF is tiny and almost insignificant. To utilize this minimal power effectively, it must be accumulated over time and then expended in a single instance. The M4 Express MCU used in previous testing consumes roughly 45 mW of power. To power this device for 10 seconds would consume 0.126 mWh of energy. At the highest measured RF power, only 3.16 μ W is produced, and it would take over 40 hours to produce this amount of energy assuming it is possible to harvest from power this low. Using ambient RF is not feasible to power this type of device, though it still may be used to power MCUs with significantly lower power requirements. For example, ultra-low-powered MCUs like the STM8L001j3 consume as little as 270 μ W [52]. To power this device for 10 seconds would only consume 0.75 μ Wh of energy, or 2.25 μ W for 30 seconds. This device is much more feasible to power with RF.

Another important consideration is the sensitivity of the system being powered. Sensitivity refers to the minimum limit of incident power required to trigger system operation. Though it is possible to collect RF energy over time, the system will not

harvest below a certain power level. The sensitivity can be calculated using equation (2) below [29].

$$\text{Sensitivity (dBm)} = 10 \log_{10}\left(\frac{P}{1 \text{ mW}}\right) \quad (2)$$

P is the minimum power the system requires to perform a task. The feather M4 express used in testing requires 0.045 W of instantaneous power to perform its tasks. Based on this power requirement, an RF harvester would require greater than 16 dBm of power to begin operation. While the Feather M4 express is a relatively power-hungry device compared to some options, this sensitivity is astronomically larger than the ambient RF available to harvest. The STM8L001j3 is one of the lowest powered MCUs on the market, requiring only 150 $\mu\text{A}/\text{MHz}$. Assuming an extremely low-power operation mode (only operating at 1MHz), the MCU requires 270 μW to operate actively. This operation puts the sensitivity at -5.7 dBm, which is still far from the amount of RF present in a typical residential scenario.

Despite this calculation, some studies have demonstrated that a much lower sensitivity can be achieved by increasing the efficiency of passive RF-DC converters. One study designed and built a rectifier that enables energy harvesting at sensitivity levels as low -40 dBm for a resistive load of 50 $\text{k}\Omega$ [50]. This sensitivity is much closer to the amount of RF energy feasibly available.

3.2 Piezoelectric

Piezoelectricity is a process that uses crystals to convert mechanical energy into electricity. By combining piezoelectric materials with floor tiles, it is possible to generate

energy from human footsteps [13], [43]. This type of energy harvesting is most applicable in areas with high amounts of foot traffic. To gauge the energy that could be harvested from human footsteps, I counted the number of people entering and exiting through a single entrance in the Elane Langone center at Bucknell.

Table 4: Number of People That Traveled Through a Single Entrance in the ELC

Time	Number of People
12:55-1:00	22
1:00-1:15	51
1:15-1:30	91
1:30-1:45	31
1:45-2:00	97
2:00-2:05	15

As recorded in Table 4, over a 1-hour period from 1:00 PM to 2:00 PM on a weekday, 270 people walked through a single entrance in the student space. In one study, an array of 20 disc-type piezoelectric transducers are placed in series and parallel to create a small tile designed to harvest energy from a single footstep [43]. The study found that an average of 60.4 mW could be harvested for every 10 footsteps. A single piezoelectric tile of this design placed in the entrance to the student space would produce 1.63 Wh during this time. This energy harvested is a significant amount compared to the 45 mWh required to power the Feather M4 Express used in testing. Though the power

produced from a single footstep is instantaneous, it can be collected and stored to power small devices, even during times of less heavy foot traffic. This strategy is only viable in spaces that get semi-regular foot traffic and may not be applicable in small residential spaces.

3.3 Heat

Thermoelectric generators (TEGs) convert heat energy into electricity using a phenomenon called the Seebeck effect: the temperature between two different semiconductors will produce a voltage between them [41]. The amount of power that is produced by a TEG is determined by the heat gradient across the hot and cold sides of the material. To model the amount of power a TEG can produce, it is necessary to measure the amount of heat that is produced by various common devices in a smart grid environment. Using an FLIR E6xt thermal imaging camera, I captured the heat signatures of some common devices. All measurements were taken with an ambient temperature of 21 °C, so I determined the heat gradient by finding the difference between ambient temperature and the heat produced by each device.

Table 5: Temperature of Common Devices

Device	Location	Temperature	Gradient
Sensor Controller System	Dana 147	31.8 °C	10.8 °C
Computer Monitor	Dana 147	40.9 °C	19.9 °C
Coffee Machine	Dana Lobby	41.3 °C	20.3 °C

TV Cable Box	Dana Lobby	38.3 °C	17.3 °C
Back of TV	Apartment	33.3 °C	12.3 °C
Projector Input Panel	Maker E	46.9 °C	25.9 °C
Security Camera	Maker E	39.3 °C	18.3 °C
Wi-Fi Router	Apartment	36.0 °C	15.0 °C

Using this information, I examined the potential performance of a compact Peltier tile, the SP1848 [42]. The open circuit potential difference between two junctions on a Peltier Thermoelectric generator are modeled by equation (3) [41], [42], [53]. In this equation, ΔT is the temperature gradient between the hot and cold sides of the tile, and α is the Seebeck coefficient: the magnitude of thermoelectric voltage generated for a specific temperature gradient across a material. The manufacturer specifications of the SP1848 provide open circuit voltages and short circuit current generated for a temperature difference of 20 °C, 40 °C, 60 °C, 80 °C, and 100 °C. Using this information, it is possible to calculate the Seebeck coefficient of the SP1848 Peltier tile.

$$V_{oc} = \alpha \Delta T \quad (3)$$

According to manufacturer specifications, a temperature gradient of 20 °C results in an open circuit voltage of 0.95V. From this, the Seebeck coefficient (α) is determined to be approximately 0.0475. Equation (4) predicts the amount of current that a TEG will produce. It is dependent not only on the resistance of the load connected, but also the internal resistance of the TEG which changes with the temperature gradient ΔT .

$$I = \frac{V}{R+R_L} \quad (4)$$

Equation (5) models the amount of power that a TEG can produce based on the Seebeck coefficient, temperature gradient, load resistance, and internal resistance [41], [53].

$$Power, P_L = \left(\frac{\alpha \Delta T}{R+R_L} \right)^2 \times R_L \quad (5)$$

The internal resistance of a TEG varies with temperature [41]. To determine the resistance through the tile at specific temperature gradients, I placed the cold side of the Peltier tile against a container of 0 °C water and exposed the hot side to a heat source until it reached the desired temperature. To ensure the cold side remained at 0 °C even as I applied the heat, I used a thoroughly mixed container of ice water. I also used the thermal imaging camera to verify the temperature gradient. Finally, I measured the internal resistance of the Peltier tile using a multimeter. Using these data, I modeled the potential produced power against the resistance of the load attached. The amount of power produced depends on the internal resistance of the MCU used. The maximum theoretical power producible occurs when the TEG internal resistance matches the load resistance.

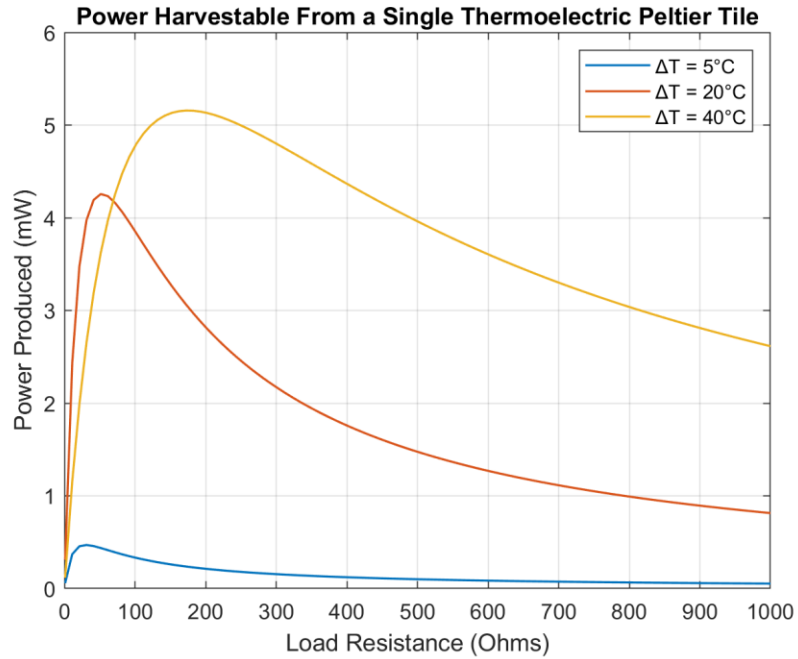


Fig. 3. Power producible by a single Peltier TEG

Although a power curve was not generated for each device's specific temperature gradient, many measured devices produced around a 20 °C difference. A single Peltier tile can produce as much as 4 mW from this amount of heat. Though this is not enough to power the M4 Express, it is plenty of power for some other low power MCUs mentioned previously.

3.4 Light

Solar PV cells work by absorbing sunlight and using that energy to generate electrical current. The power output of solar panels is typically measured in 1000W/m² conditions. This solar intensity usually only occurs in the middle of the day in direct sunlight when the sun is at its highest and brightest point. "While ambient power

generation using solar power is a strong candidate to consistently generate energy throughout the year, indoor lighting is said to be equal to only 1/100 – 1/1000 of the daytime outdoor sunlight brightness. Therefore, indoor photovoltaic power generation using indoor lighting has low output [37].” However, a significant amount of energy can also be harvested in indoor conditions with a PV cell mounted in a window. In their evaluation of indoor PV power generation, C. A. Reynaud et Al. had the following to say: “Indoor light differs from outdoor light in three considerable aspects: i) the light spectrum is different from the solar spectrum and depends on the nature of the source itself (Halogen, LED, CFL...), ii) irradiances are typically in the range of 0.1 – 1 mW/cm², much lower than 100 mW/cm², and iii) indoor light also rarely falls solely under direct normal incidence on the solar cells, but instead features both an oblique direct component and an isotropic diffuse component” [54].

For this reason, I did not rely on indoor lights, but rather harvested the sun from an indoor environment. In the following tests, I gathered data using a small 25 cm² high-efficiency monocrystalline PV cell. Using a series of resistors, I created IV curves for this cell in different lighting conditions. Using an Extech Instruments LT300 light meter, I measured the ambient light intensity. As a baseline measurement, I recorded 80.6 kLUX at 1:09 PM on a sunny day with few clouds in the sky. I use this measurement as an approximation to the 1000 W/m² ideal testing conditions. Fig. 4 shows the results.

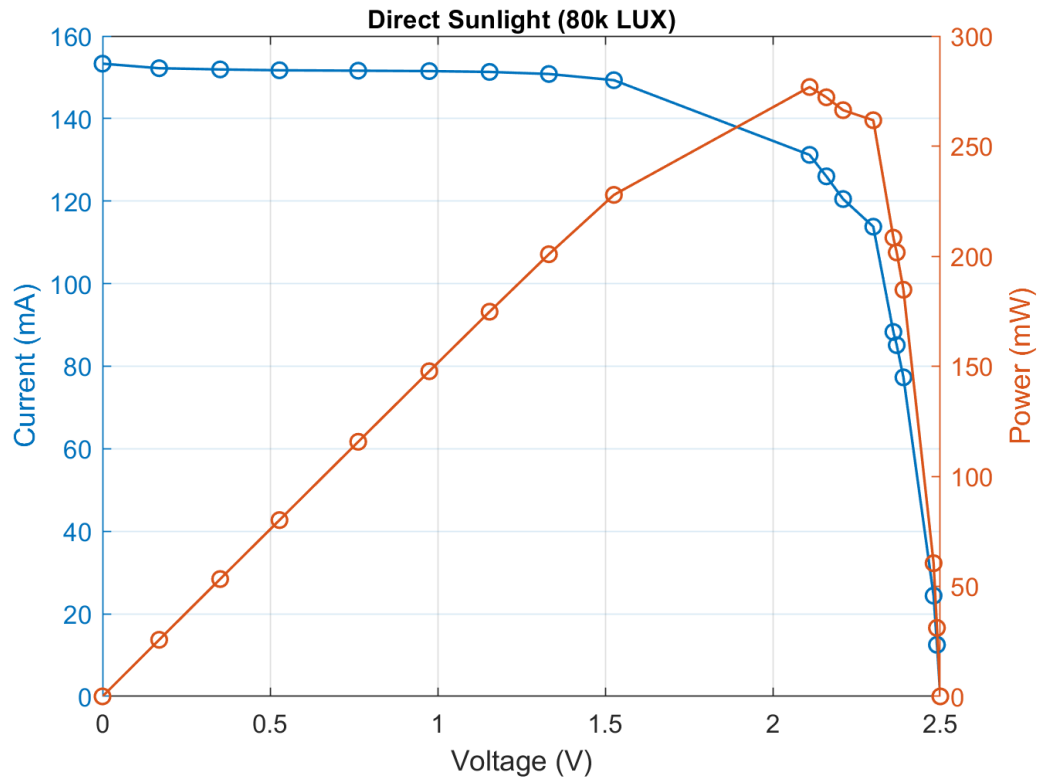


Fig. 4. IV curve in direct sunlight

Next, I created an IV curve for the cell in indoor conditions when attached to a south-facing window. Over 80% of Earth’s population lives in the northern hemisphere, therefore most of earth’s population receives a majority of sunlight from south facing windows. As expected, using the cell in a south-facing window produces a significant percentage of the power produced in direct sunlight, roughly 50%.

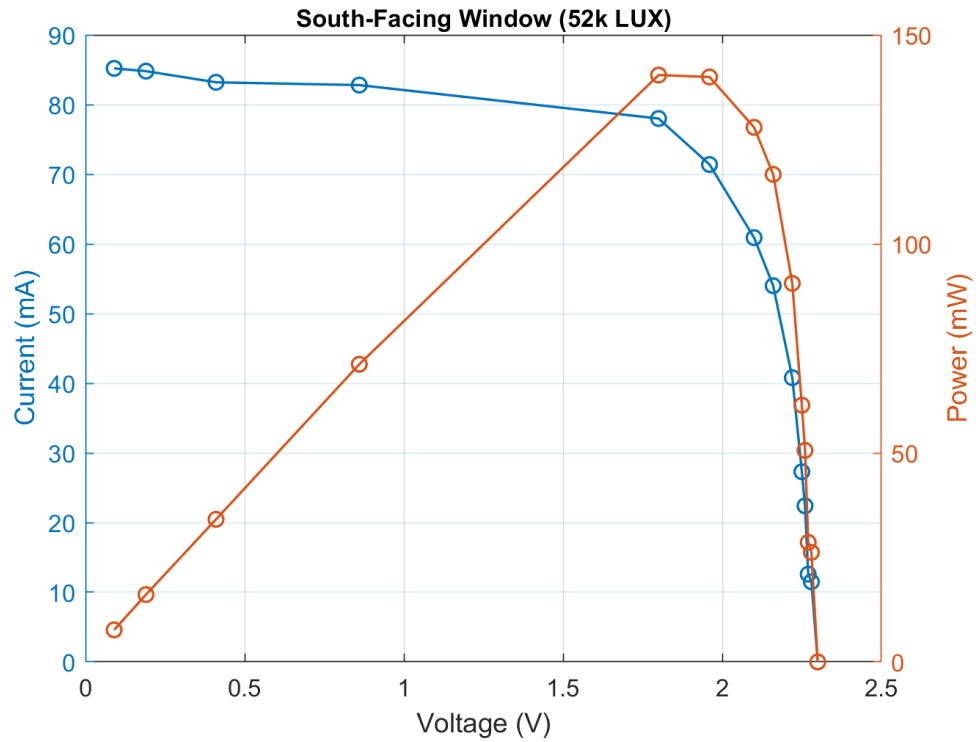


Fig. 5. IV curve for south-facing window

Comparing the data, the most practical implementation of PV harvesting in microgrid is to place a high-efficiency monocrystalline cell in a south-facing window. Even a single 25 cm² cell can produce over 100 mW, which is enough to power many low-power MCUs. Meanwhile the drop in power produced when comparing this to a north-facing window or even lower indoor lighting conditions is drastic, almost 98%.

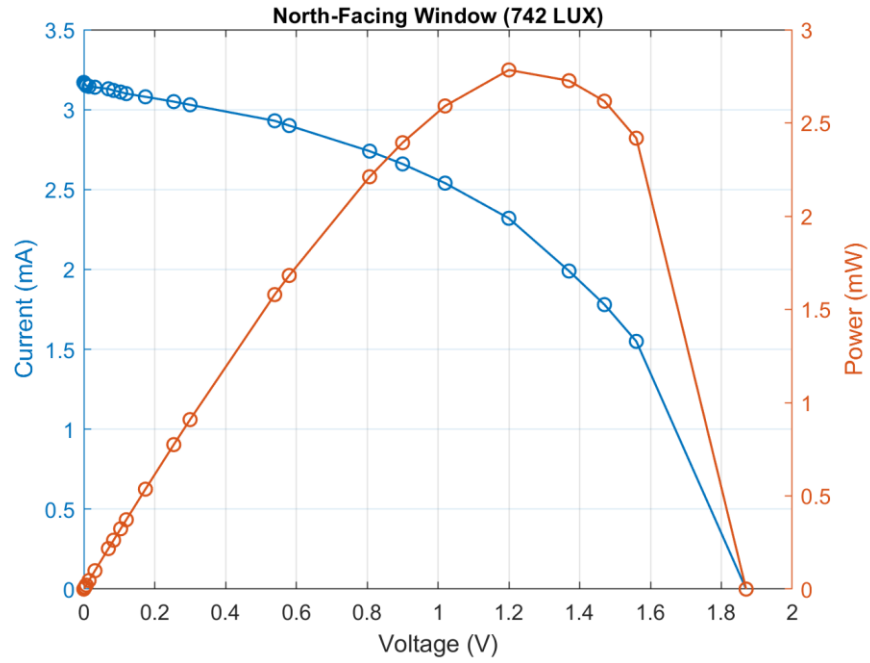


Fig. 6. IV curve for north-facing window

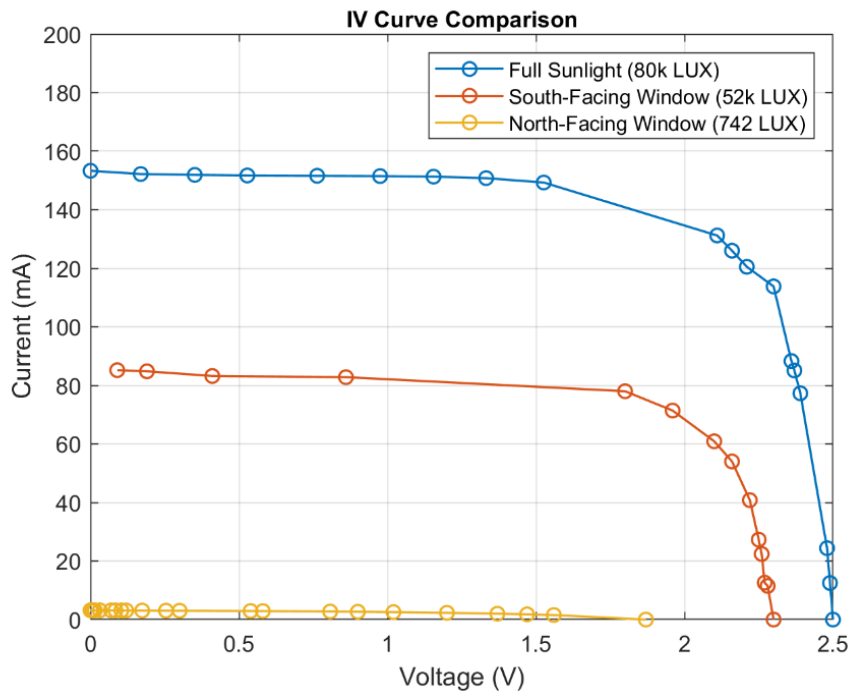


Fig. 7. IV curve in different lighting conditions

A significant amount of energy can be harvested from a south-facing window. Two of these small monocrystalline cells could power an Arduino, a relatively power-hungry MCU. A single PV cell in a south-facing window produces plenty of power for the M4 Express. While this high-density energy is only available when the sun is out, because of its abundance, it could be easily stored to indefinitely power the M4 Express MCU. Even the PV cell placed in the north-facing window produces power on par with a single Peltier tile and would be capable of powering an 8-bit MCU like the STM8L001j3.

To harvest energy when the sun is unavailable, it is possible to harvest light energy from indoor lights. Because these lights broadcast a much smaller portion of the light spectrum than the sun, only a fraction of the power harvestable from the sun can be produced. In a well-lit indoor space, the light meter measured 731 Lux, which is comparable to the amount of light measured in a north-facing window. Though due to differences in the spectrum, the power producible from indoor light is expected to be less. The amount of power that can be produced from this method is also highly dependent on the PV cell's distance from the source and the angle of incidence of the panel. One study examines these relationships more closely [54].

3.5 Source Comparison

The SP1848 TEG demonstrates the ability to generate approximately 4 mW of power when exposed to a 20 °C temperature gradient. Meanwhile, a single 25 cm² high-efficiency monocrystalline PV cell can generate nearly 150 mW when placed in a south-facing window, which is about half of its maximum output under direct sunlight.

Although this energy source is limited to daylight hours, excess energy can be stored in a

battery or supercapacitor for continuous sensing. However, when comparing the power produced in a north-facing window or under lower indoor lighting conditions, there is a dramatic 98% reduction in output. Despite this difference, the PV cell in the north-facing window still produces power comparable to a single Peltier tile. In high foot traffic areas, a single piezoelectric tile can generate 1.63Wh of energy during an hour, which is substantial. While the power produced from each footstep is momentary, it can be accumulated and stored to power small devices during periods of lighter foot traffic. Ambient RF energy harvesting yields an almost negligible amount of power. To use this minimal power, it must be captured over an extended duration.

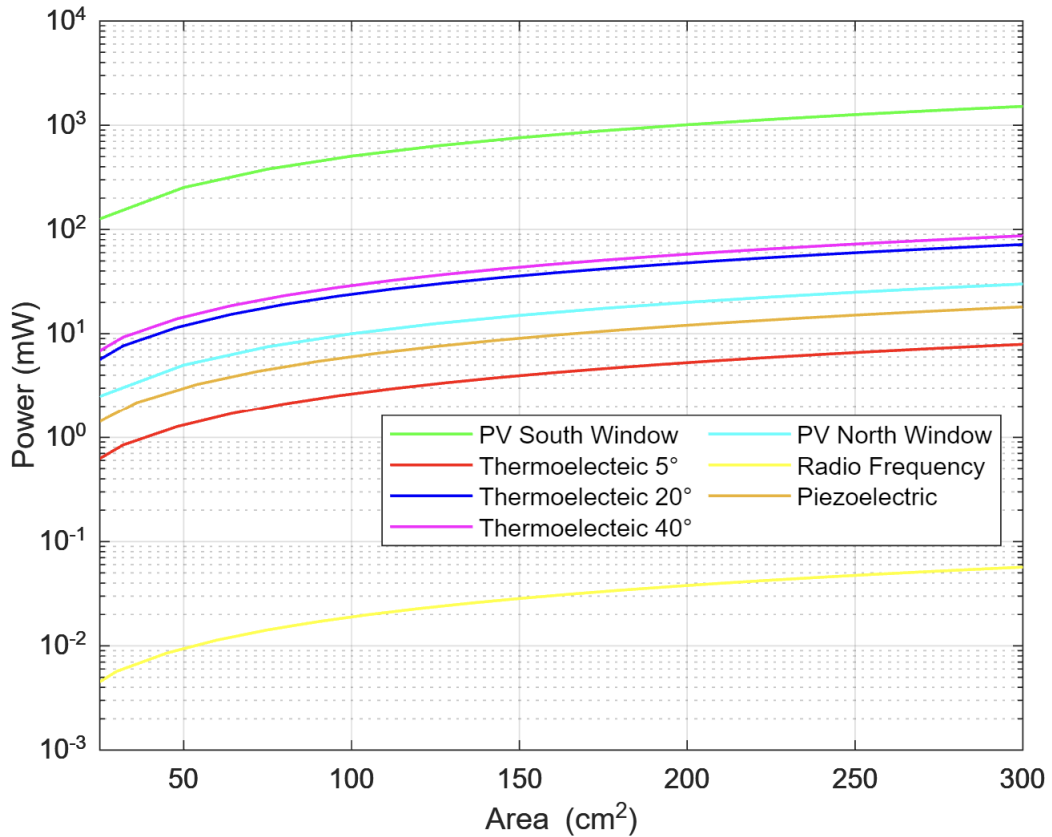


Fig. 8. Ambient energy sources compared on a logarithmic scale

Based on the collected data, thermoelectric and PV harvesting emerge as the most viable options for wireless home energy management sensors. PV technology, particularly when deployed in a south-facing window, boasts the highest energy density among the tested sources. Despite limited harvestable hours due to sunlight availability, its substantial energy density makes it a clear choice. Additionally, thermoelectric harvesting proves promising, given its relatively high energy density and the abundance of heat sources and gradients in residential spaces.

Conversely, RF and piezoelectric harvesting are excluded from further consideration. While piezoelectric technology can yield significant energy from human footsteps, its practicality relies on consistent foot traffic, which does not align with the residential context. Likewise, RF harvesting, despite continuous energy generation, provides minimal power output, limiting its practical application. Although it may find niche uses in specific scenarios, such as intentional RF energy beaming or environments with high RF interference, its overall suitability for integration into home energy management systems is constrained.

In conclusion, the decision to focus on thermoelectric and PV harvesting is grounded in their superior energy density, availability, and consistent performance, making them optimal choices for wireless home energy management sensors.

Chapter 4: Harvester Design

4.1 Feasibility Study

4.1.1 Proving the Initial Hypothesis

Prior to delving into a thorough examination of components or system architecture, I addressed a fundamental hypothesis question upon which my research is predicated: can ambient energy harvesting accumulate sufficient energy for data transmission? Given that the energy required for transmission is 5–6 or more times higher than for other operations [33], the viability of the system hinges on whether it can amass this level of energy; failing to do so would render the system ineffective.

The feasibility study incorporated several key elements. At a basic level, the system required a transducer for energy harvesting, a switching converter for voltage regulation, a capacitor for voltage storage, and a transmitter for data communication. To maximize energy density for the system, a small monocrystalline PV cell was chosen as the transducer. The setup used an Xbee S1 transmitter and an LTC3108 energy harvesting IC for the experiment. The reasoning behind selecting these specific devices is detailed in a later section. Additionally, a 2N7000 n-channel MOSFET was employed to connect the transmitter to the ground, with its gate linked to the voltage monitor on the LTC3108, enabling data transmission once the capacitor had sufficiently charged.

Based on the energy consumption data for the Xbee S1 provided in its datasheet, I determined a suitable range of capacitor sizes. While there isn't a single "best" size for the capacitor, multiple design considerations need to be taken into account. As the

transmitter starts consuming current from the capacitor, the voltage decreases quickly. Although transmitters can tolerate some variation in input voltage, there's a threshold below which the transmitter fails to function properly. It is necessary to select a capacitor size that ensures a sufficient amount of energy is available for the transmitter's use. Energy remaining in the capacitor becomes unusable once the voltage falls below the transmitter's minimum operational threshold.

An additional consideration in the design process is the duration for which the transmitter must remain active, which is contingent upon the transmission length. At this stage of the project, the exact message length required by the system was undetermined. Consequently, I compiled a table correlating various capacitor sizes with the corresponding operational time they would permit for the transmitter. By assessing the transmitter's data rate, it is possible to determine the message length that can be supported by each capacitance value.

Table 6: Effect of Capacitor Size on RF Transmitter

Capacitor Size	Allowed Transmission Duration for 1.5 V acceptable drop (ms)	Message Length (b) (calculated for 250 kbps)
100 μF	3	750
470 μF	14.1	3525
1000 μF	30	7500
2200 μF	66	16500
2670 μF	80.1	20025

Though these calculations do not include the startup time of the transmitter, I was reasonably confident that a 2670 μF capacitor would be sufficient for a very basic transmission. For the system to operate correctly, the output capacitor should not be directly connected to the transmitter load. This arrangement leads to an issue known as the cold start problem [44]. The capacitor charges up to the minimum voltage needed for the transmitter to start consuming power. However, the moment it begins drawing current, the capacitor ceases to charge further, hindering its ability to accumulate the energy needed for transmission.

To overcome this issue, an automatic switching mechanism is required to temporarily disconnect the transmitter until the output capacitor is adequately charged. The LTC3108 includes a voltage monitoring feature. Its “PGD” or “power good” pin, initially low, shifts to high when it senses the output capacitor has reached 90% of its full charge. This pin can be connected to the gate of a MOSFET which in turn connects and disconnects the transmitter and output capacitor. In my experiments, I started with a 2N7000 n-channel MOSFET from ON Semiconductors. Although it was functional, the gate-to-source voltage threshold was unexpectedly high, which limited its effectiveness. The MOSFET also drew unwarranted current from the main capacitor. Switching to the integrated P-channel MOSFET within the LTC3108 significantly enhanced the system’s performance.

The LTC3108 features a secondary voltage output, labeled Vout2 or OU2. As Output 1 gradually charges the capacitor, the secondary output stays isolated from the system. It remains so until the Ven (enable) pin is activated high, at which point it bridges both outputs. This setup allows the Vdd pin of the transmitter to be connected to this

second output, ensuring it stays disconnected from the energy source until ready. This arrangement permits the capacitor to continue charging until the secondary output is activated.

The Xbee S1 was set up to transmit a digital high signal, which was then replicated at a secondary Xbee receiver. The system efficiently powered the transmitter, and the high signal was successfully detected by the receiver. Although no sensors were connected, this proof-of-concept validated that enough energy could be harvested to energize the system's most power-intensive component. The illustration in Fig. 9 helps demonstrate the expected voltage across the capacitor (C_s) in this proof-of-concept setup.

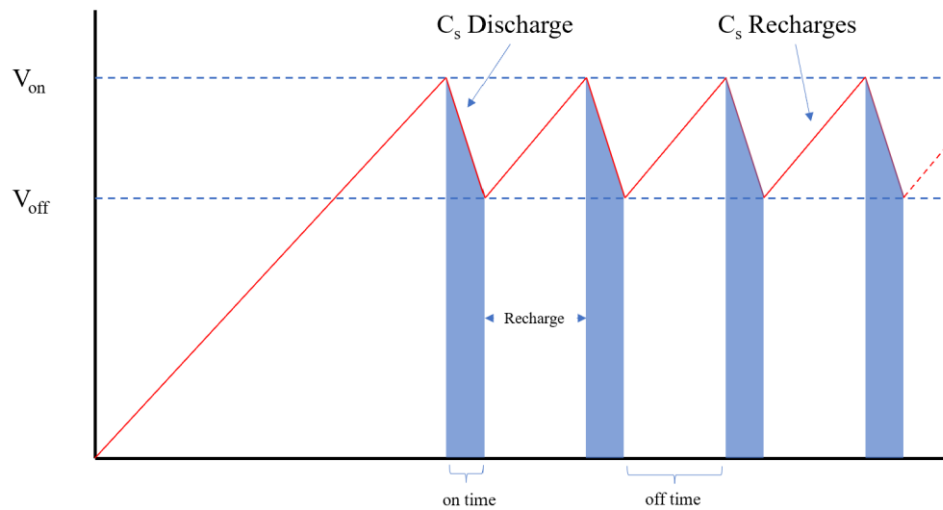


Fig. 9. Expected capacitor voltage behavior for feasibility study

While this version of the system works, it presents several problems regarding the consistent transmission of data. The system charges the output capacitor using the harvesting source and transmits as soon as the capacitor has enough voltage. Therefore,

the capacitor immediately dumps out all its charge as soon as it is full, leaving no time for harvested energy to be stored in a long-term storage medium.

This method of transmitting immediately when sufficient energy is collected simplifies the system and is appropriate for certain applications where the harvesting source is continuously available, such as in [23] and [44]. However, for PV harvesting where energy is only available with sunlight, the system will cease to function during night hours.

What I propose is a more intelligent system that only transmits data when absolutely essential. As discussed earlier, data transmission consumes an order of magnitude more energy than any other function in the system. Therefore, it is logical that minimizing data transmission is the key to saving the most energy. A system that is not constantly transmitting also allows unused energy to be stored for periods when the energy source is unavailable. The illustration in Fig. 10 shows the proposed functionality of this more intelligent system.

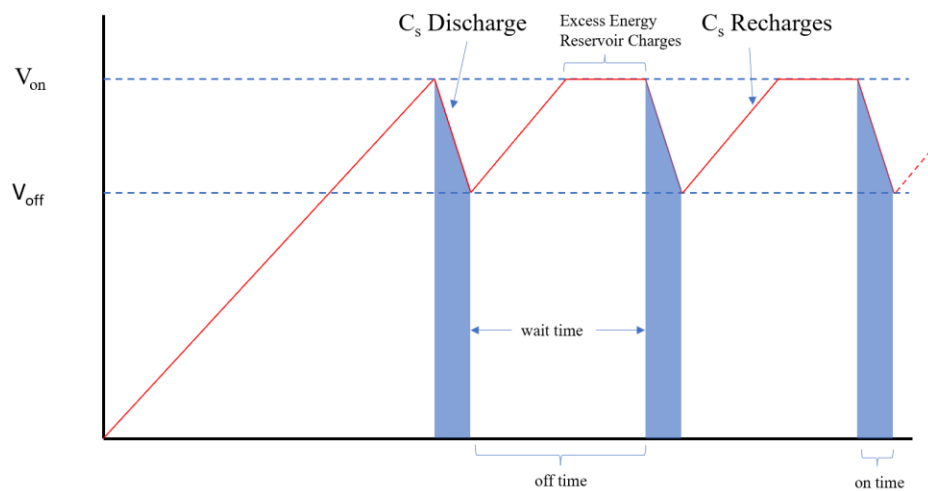


Fig. 10. Proposed capacitor voltage behavior for energy-aware system

4.1.2 Excess Energy Reservoir

As explored in the preceding section, the communication module represents the primary power consumption element within the system, necessitating the selection of a main output capacitor that can sufficiently support the energy demands of this component. Several considerations and assumptions come into play when selecting an appropriate capacitor for the output. As the capacitor rapidly discharges, its voltage also decreases. Once the capacitor falls below a certain voltage threshold, it becomes incapable of supplying energy to the transmitter module. The determination of an acceptable voltage drop is the initial step, contingent on the specific transmitter. It is prudent to establish the maximum allowable drop based on the transmitter's low voltage threshold—the lowest voltage at which it remains operational. Should the voltage dip below this threshold, functionality ceases.

Another consideration involves the trade-off between capacitor size and energy storage. A larger capacitor can store more energy, enabling extended communication periods. However, a larger capacitor necessitates a lengthier charging time.

Designing for this scenario can be approached in a few ways. Firstly, one can select a capacitor and allowable voltage drop, subsequently calculating the potential duration of active communication. However, this method lacks efficiency as it disregards the actual time required to transmit data. Alternatively, if the transmission duration and peak current consumption are known, one can start with this information and select an appropriate capacitor that sustains peak current for the specified duration without falling below the allowable minimum voltage.

4.1.3 Long Term Storage: Battery vs. Supercapacitor

An excess energy reservoir needs to be chosen to store energy for the system to use when the harvesting source is unavailable. Traditional WSN nodes might use a rechargeable lithium-ion battery. Though a battery could be used for this application, one of the benefits of using energy harvesting to power sensor nodes is mitigating reliance on battery technology [28], [29], [30]. “As electronics became smaller and required less power, batteries could grow smaller, enabling today’s wireless and mobile applications explosion. Although economical batteries are a prime agent behind this expansion, they also limit its penetration; ubiquitous computing’s dream of wireless sensors everywhere is accompanied by the nightmare of battery replacement and disposal” [28]. I therefore propose that a supercapacitor can provide sufficient energy to the sensor node.

Some preliminary calculations reveal the amount of energy that can realistically be stored. I assumed 7 hours of harvestable sunlight and that the IC produces a typical output of 4.5mA (indicated in the datasheet) [55]. I chose a capacitance of 4860 μ F to power the transmitter: the calculations to arrive at this result are explored further in the “4.5.3 Xbee S1 Analysis” section.

There is no series resistor intentionally placed in the system, however approximate internal resistance of the supply can be calculated by using the average current output and ohms law.

$$R = \frac{V}{I} = \frac{3.3V}{4.5mA} = 733.3 \text{ ohms} \quad (6)$$

With the collected information, it is possible to estimate the amount of time it takes the output capacitor to charge in between bursts.

$$V_c(t) = V_s(1 - e^{(-\frac{t}{RC})}) \quad (7)$$

$$t = 2.92 \text{ seconds (charge to 1.9 V)}$$

$$t = 5RC = 17.82 \text{ seconds (full charge)}$$

$$\Delta t = 17.82 - 2.92 = 14.9 \text{ seconds from 1.9 V to 3.4 V}$$

For the next section, I am assuming that transmission happens at a wide, but reasonable, interval of 10 minutes or 600 seconds.

$$\text{charge time per cycle} = 600 \text{ s} - 14.9 \text{ s} - 201 \text{ ms} = 584.9 \text{ s}$$

97.4% of each cycle is spent charging the long term storage

$$0.974 * 7 \text{ hours} = 6.824 \text{ hours can be spent collecting energy}$$

With this information, it is possible to calculate the size of a lithium-ion battery that can be charged in this amount of time.

$$\text{charge time} = \frac{Ah}{A} \quad (8)$$

$$6.824 \text{ hours} = Ah / 4.5 \text{ mA}$$

Given the outlined assumptions, the system can charge a battery with a capacity of 30.7 mAh over the course of a day. This approach allows for calculations of the battery's energy storage capacity and its implications for the system's operational duration once the transducer ceases energy supply.

$$E = V * Ah \quad (9)$$

$$E = 3.7 \text{ V} * 30.7 \text{ mAh} * 3600 = 409 \text{ J}$$

This charge translates to 21,171 times the amount of energy stored in the 4860uF output capacitor.

$$E_{harvest} = \frac{C_s}{2} (V_{on}^2 - V_{off}^2) = \frac{4860 \mu F}{2} (3.4 V^2 - 1.9 V^2) = 19.3 mJ \quad (10)$$

$$\# \text{ of charges at output} = \frac{409 J}{19.3 mJ} = 21,171 \text{ times}$$

Assuming a 10-minute cycle per operation, this results in 3,528 hours of system functionality. This same calculation can now be applied to a supercapacitor instead of a lithium-ion battery. In contrast to the main output, the supercapacitor charges up to 5V. A recalculation of the internal resistance gives R = 1111 ohms. Equation 11 provides an approximation for the time it takes a capacitor to fully charge.

$$t = 5RC \quad (11)$$

$$6.824 \text{ hours} = 24566.6 \text{ seconds} = 5 * 1111 \text{ ohms} * C$$

$$C = 4.42 F$$

$$E = \frac{4.42}{2} (5V^2 - 3.3V^2) = 31.2 J$$

$$\frac{31.2 J}{19.3 mJ} = 1616.4 \text{ charges}$$

Within the timeframe of sunlight suitable for energy harvesting, a 4.42 F supercapacitor can be charged, holding 1616 times the energy of the output capacitor. Given a 10-minute transmission cycle, this amounts to 269.4 hours of operation. Therefore, a supercapacitor can provide sufficient energy to support this system effectively.

4.2 Prototype Design

Using what I learned from the feasibility study, I refined the harvester design. I developed a microgrid, energy-harvesting sensor according to the block diagram in Fig. 11. Its energy harvesting aspect is similar to designs explored in [8], [10], and [11]; however, the proposed hybrid system seeks a balance between device lifetime and performance by using harvested energy to power the radio and separately powering the MCU and sensors with a small coin-cell battery.

In the energy harvesting chain, initially, a transducer gathers energy from the environment. The system supports any DC source capable of generating power above the minimum threshold required by the energy harvesting IC module. For experimental purposes, data from the system was obtained using a PV cell.

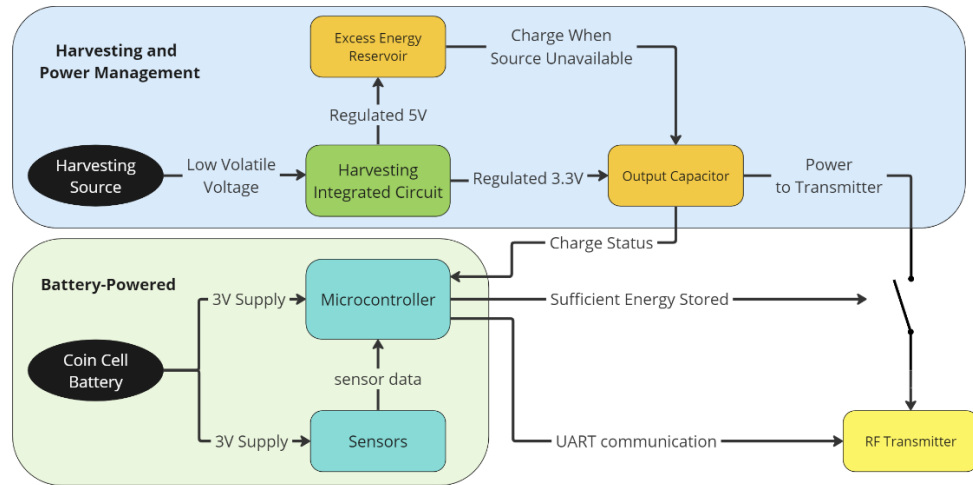


Fig. 11. Hybrid battery and energy harvesting system block diagram

An energy harvesting IC boosts and regulates the transducer voltage which in turn charges an electrolytic capacitor. When this main capacitor is fully charged, a

supercapacitor stores any additional energy, acting as an excess energy reservoir. This stored energy powers the radio communication subsystem when the main ambient energy source is unavailable.

A low-power MCU monitors the charge status of the main capacitor and collects data from external sensors. The system uses two sensors, an analog temperature sensor and a digital passive infrared (PIR) occupancy sensor. To save energy and limit the number of radio transmissions, the MCU enters a low power mode for a fixed duration between active cycles. Upon waking into active mode, the MCU checks the charge status of the output capacitor and reads the sensor data. If sufficient energy is stored in the output capacitor, the MCU sends packetized sensor data via UART to the radio module for RF transmission, rapidly discharging the capacitor in the process. After transmission has ended, the RF transmitter disconnects allowing the capacitor to resume charging. If the transducer stops providing sufficient power to charge the capacitor, it charges from the excess energy reservoir instead.

While the MCU and sensors can be powered from the Low Dropout Voltage Regulator (VLDO) housed within the harvesting IC, powering these components separately with a small 3 V coin-cell battery frees up the capability of the harvester allowing it to operate more efficiently. Thus, the communication system is powered from ambient energy while sensing and supervisory functions are powered by an external coin cell battery.

The following details a proof-of concept system developed for the proposed design. Because the design is modular, any of the specifically chosen components could be swapped out to accommodate the specific needs of an end user.

4.2.1 Harvester Choices

Harvested energy is volatile and typically needs to be boosted and regulated.

While a simple switching converter may suffice in some cases, utilizing chipsets intended for energy harvesting applications provides better coverage [31].

Table 7: Commonly Used Energy Harvesting ICs

Device	LTC3105	TI BQ25504	LTC3108
Voltage Output	1.6 V to 5.25 V	Up to 5 V	2.35 V, 3.3 V, 4.1 V, 5 V
Viable Sources	Solar	Solar, TEG	Solar, TEG
Vin Range	225 mV to 5 V	≥ 600 mV	20 mV to 500 mV
LDO (2.2V)	6 mA	N/A	3 mA

4.2.2 LTC3108 Analysis

Due to its availability, features, explicit compatibility with both PV and thermoelectric sources, and adjustable output voltage, the Linear Technologies LT3108 was selected [13]. While this device is deemed most suitable for this application, any compatible IC can be used without significant impact to the overall design.

The LTC3108 is connected in its typical configuration according to the datasheet. In this configuration, the LTC3108 can harvest from as little as 20 mV and provides

boosted, regulated outputs. While the minimum DC operating point is 20 mV, the operating characteristics change quite a bit when a load is introduced. To harvest from such low voltages and maintain performance, the LTC3108 converts the DC input to an AC signal, using a 1:100 transformer to boost the voltage before conversion back to DC at the output. Multiple conversions negatively impact efficiency with varying loads degrading it further. Fig 12. illustrates how efficiency rapidly drops as the load pulls more current from the output. Efficiency data was collected using two NGU201 source measure units (SMUs).

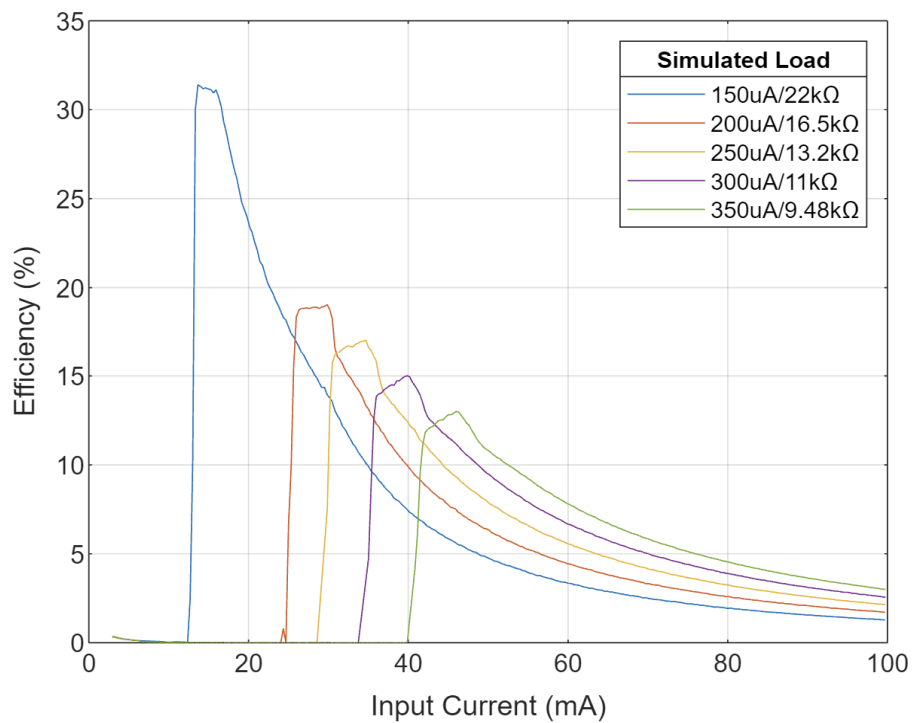


Fig. 12. Measured efficiency curves for power management boost converter

One SMU connected to the input of the LTC3108 circuit swept current from 3mA up to 100mA. A second SMU connected to the output of the LTC3108 performed a load pull measurement. Each SMU collected data every 100ms. Fig. 12 shows this data.

In another test, the SMU measured the minimum harvesting voltage and current of the LTC31308 with no load connected, revealing that the minimum DC operating point of the IC is 19.81 mV and 1.998 mA or 39.58 μ W. The load on the LTC3108 needs to be minimized to take advantage of this high harvesting sensitivity.

4.3 Low Power Microcontrollers

4.3.1 Microcontroller Choices

The system includes a low-power MCU to monitor the charge status of the output capacitor as well as read and send sensor data to the transmitter. Table 8 shows the consumption of selected commonly used MCUs as reported by their datasheets.

Table 8: Commonly Used Low-Power Microcontrollers

Device	MSP430G2553 [56]	PICF1503 [57]	STM8L001J3 [52]	STM8L050J3 [58]
Operating Voltage	1.8 V to 3.6 V	2.3 V to 5.5 V	1.8 V to 3.6 V	1.8 V to 3.6 V
Active mode	230 μ A at 1 MHz	30 μ A at 1 MHz	150 μ A at 1 MHz	150 μ A at 1 MHz
Sleep	0.5 μ A	0.02 μ A	0.8 μ A	0.8 μ A

Once again, the considerations of compatibility and ease of use significantly influenced my selection of a microcontroller. While STM MCUs are among the lowest power options available, the process of setting them up with written code proved to be

exceptionally challenging. Flashing code to STM chips requires the use of STM's dedicated programmer, the "ST-Link." In my testing, I utilized an ST-Link V2 for these 8-bit MCUs, which employ a single-wire interface known as SWIM. Although STM MCUs support languages like C and C++, the programming software, ST Visual Programmer (STVP), poses challenges in terms of usability and configuration. An alternative option, IAR System's Embedded Workbench for STM8 Microcontrollers, offers a user-friendly interface but requires a recurring subscription. While configuring Visual Studio Code to use OpenOCD for programming STM devices is possible, gathering the required dependencies for STM8 MCUs presented challenges. The documentation for these 8-bit microprocessors appears to be less comprehensive compared to some of STM's other devices, possibly owing to the more niche nature of their application. In my testing, programming the devices proved elusive until I identified a driver conflict that had hindered the interaction between the programmer and the MCU. Additionally, it is noteworthy that without adding a specific delay in the code during the initial programming, subsequent reprogramming becomes impossible.

4.3.2 MSP430G2553 Analysis

The proposed system uses the 16-bit Texas Instruments MSP430G2553. This MCU family boasts well-documented features, consumes minimal energy, and incorporates a relatively intuitive programming environment and toolchain [44].

The MSP430G2553 16-bit microcontroller measures data from external sensors and monitors the charge status of the output capacitor. It then determines when the system should transmit. With its current programming, the MSP regularly enters and exits low power mode to consume as little energy as possible.

The MSP430G2553 has six power modes [56]. In Active mode, the CPU is active and all enabled clocks are active. In Low Power Mode zero (LPM0), the CPU is turned off, which means it is not executing code. However, the MCLK (Main Clock) is also disabled, while the SMCLK (Sub-Main Clock) and ACLK (Auxiliary Clock) remain active. This functionality allows peripherals that rely on these clocks to continue operating while the CPU is inactive, thus conserving power while waiting for an event that requires the CPU's attention. LPM1 or timer mode is similar to LPM0 with both the CPU and MCLK turned off. Additionally, the digitally controlled oscillator (DCO), which can be a source of the MCLK, is disabled unless it is sourcing the ACLK. The ACLK remains active, which allows timer-based peripherals to run, such as those that might be used for real-time clock features. In LPM2 or standby mode, the CPU, MCLK, SMCLK, and DCO are all disabled. The DC generator, however, remains enabled, and the ACLK remains active. This mode is typically used when the application needs the DC generator to be ready for a quick start-up, but the CPU and main clocks can be turned off to save power. In LPM3 or sleep mode, the CPU, MCLK, SMCLK, DCO, and the DC generator are all disabled, with only the ACLK remaining active. This mode offers deeper power savings compared to LPM2 because it shuts down more system clocks, including the DC generator. It is used in scenarios where power conservation is paramount and the longer wake-up time that results from having to restart the DC generator is acceptable. Finally, in LPM4 or off mode, all the clocks including the ACLK are disabled. The MCU is essentially in a deep sleep state and can only be woken up by an external interrupt. LPM3 is the lowest power mode where the MSP430 can still wake itself without an external interrupt.

Benchtop measurements revealed that at 3.3V, the MCU consumes 369.2936 μA in active mode and 0.41 μA in LPM3.

4.4 Sensors for Microgrid IoT

Careful consideration must be given to the selection of sensors to ensure compatibility with the low-power system. The LTC3108 is equipped with multiple regulated outputs, featuring a main output with a configurable voltage. This main output gets connected to a capacitor that undergoes a gradual charging process, subsequently enabling the connection of the load once it collects an appropriate amount of energy. Such a mechanism facilitates the accumulation of a higher amount of energy over time compared to instantaneous harvesting from the sources.

This approach is necessary for the communication module, which doesn't require continuous power but demands an order of magnitude higher energy input than other system components. Although it is feasible to power sensors with this output, such an approach is neither necessary nor practical. Unlike the communication module, which can be powered on and off as needed, sensors should operate continuously to generate a comprehensive understanding of the measured space. Continuous operation is crucial, especially for sensors measuring occupancy that require regular environmental checks. Intermittent powering on and off could lead to inaccurate readings.

Furthermore, the LTC3108 offers an additional output featuring a Low Dropout (LDO) Regulator, maintaining a steady 2.2V output and capable of providing up to 3mA (source dependent). This output proves ideal for powering sensors and any other components that require continuous operation. The careful selection of sensors is

imperative to ensure their reliable operation when powered by the LDO output or by a small coin-cell battery.

4.4.1 Chosen Sensors

Of the different types of sensors used in home energy management and microgrid systems, occupancy and temperature sensors provide the most practical utility. The most valuable information for load management is detecting if a resident is present. If there is no one present, the maximum amount of energy can be saved by simply powering off every unused device [59]. Meanwhile temperature data is important for evaluating the comfort of an environment. HVAC systems consume a lot of energy and environmental temperature information is essential to minimizing their usage while maintaining the comfort of the resident [6].

T. Ishiyama underscores the importance of environmental data for optimizing energy management systems: “Electronic devices and other terminals need to transmit information about themselves, such as remaining battery capacity, as well as information about the surrounding environment, such as temperature and humidity, to the network.” This data is vital not just for system performance but also for the sustainability of network operations, reinforcing the choice of temperature sensors as a critical component [37]. Similarly, the research by L.-G. Tran, H.-K. Cha, and W.-T. Park into smart grids reveals how temperature and occupancy data play a crucial role in balancing power demand with supply, especially during peak times. Their work shows how automated HVAC systems, guided by sensor inputs, can significantly contribute to energy savings while maintaining user comfort [29].

Moreover, H Pavana and Rohini Deshpande's exploration into household energy conservation strategies highlights the broader utility of sensors. By employing piezoelectric tiles and solar tracking systems alongside IR and LDR sensors, they demonstrate how automated control based on sensor data can lead to substantial energy savings. This approach, particularly in managing lighting based on occupancy and ambient light levels, exemplifies the practical benefits of integrating sensor technology into energy management systems [30].

The collective insights from these studies validate the selection of occupancy and temperature sensors for their direct influence on system efficiency and energy conservation. By continuously monitoring environmental conditions, these sensors enable smarter, more responsive microgrid solutions that not only optimize energy usage but also regulate the living comfort of residential spaces.

4.4.2 Temperature and Occupancy Sensor Analysis

For occupancy, the system uses an EKMB1103113 PIR sensor from Panasonic. For temperature the system uses an MCP9700A-E/TO Low-Power Linear Active Thermistor IC from Microchip Technology. Using an SMU to measure the current draw of these devices at 3.3 V over a period of 10 minutes reveals that the PIR consumes 0.9109 μA and the temperature sensor consumes 5.6246 μA on average. In a 24-hour period, the sensors collectively consume 1.694 J of energy at 3 V.

4.5 RF Transmitter

The RF transmitter adds another level of complexity over the previously discussed system loads. Communication modules consume several orders of magnitude

more power than any other component in the system: “The power consumed during transmission is 5–6 times greater than that consumed by other tasks” [33]. Choosing an appropriate transmitter that draws the lowest amount of power is important, but minimizing communication time is also important. Table 10 shows some commonly used and low power communication modules that could be easily integrated into the harvesting sensor’s design.

4.5.1 Communication Protocol

In their study of applications of wireless communication technologies in microgrid, Shivangi Verma and Poonam Rana also directly compare different wireless communication technologies [7].

Table 9 Wireless Communication Technologies Compared [7]

Wireless Technology	Data Rate	Coverage Area	Application for Smart Grid
WLAN	1-54 mbps	100 m	Communication aided line protection, enhanced transformer different protection
ZigBee	20-250 kbps	10-100 m	Control for home appliances, Direct load control
Cellular	60-240 kbps	10-50 km	SCDA interference remote distribution substation

WiMax	70 mbps	84 km	Automatic Meter Reading (WMAR), Real Time Pricing
Bluetooth	721 kbps	1-100 m	Local online monitoring application

The final prototype system uses the ZigBee standard. While alternative low-rate communication protocols such as BLE, Z-wave, or LoRaWAN present viable options, the selection of ZigBee is predicated on its intrinsic design for short-range communication, adept penetration of obstacles, flexible configurability, and widespread integration into existing IoT platforms. This ubiquity facilitates seamless integration with established systems.

Each ZigBee device is endowed with a unique 64-bit IEEE address, assigned during the manufacturing process. This address serves as a digital identifier, ensuring precise data delivery to the intended recipient within the network. Furthermore, ZigBee allows for the utilization of 16-bit short addresses, streamlining the addressing process and mitigating the overhead associated with lengthier addresses. This unique addressing capability enables devices to communicate directly with each other or leverage intermediate nodes for relaying information. While ZigBee devices can be configured into a mesh network, the testing methodology employs peer-to-peer communication between two devices. “Currently, Zigbee is the leader in monitoring and control products to manage energy and water. The Zigbee Smart Energy profile is one of the main areas in development in recent years for energy efficiency. Furthermore, this profile is complemented with other profiles such as Building Automation, Home Automation or

Light Link” [3]. “[Compared to the] Zigbee (IEEE 802.15.4) wireless network..., Wi-Fi sensors are more difficult to implement requiring a network stack and security to be implemented – increasing the complexity” [1].

4.5.2 Some Transmitter Options

Table 10 shows RF modules that were considered for the prototype energy harvesting sensor. To send data, the final system uses an Xbee S1 RF module from Digi International configured to transmit via the ZigBee standard [60]. This reasoning behind and performance of this transmitter is further explored in the next section. It is worth noting that the Xbee S1 is no longer available, however the Xbee S2 is still in production and has nearly identical specifications.

Table 10: Explored Transmitter Options

Device	Core51822 (based on nRF51822)	BlueFan BH678 BLE	TWE-L-DI-P	Xbee S1	MRF24J40MA-I/RM	ATZB-X0-256-3-0-CR
Type	Communication and sensing SOC	SoC with integrated antenna	RF module	RF module	RF module	SoC with integrated antenna
Sleep Current	2.6 μ A at 3 V ON mode, all blocks IDLE	< 0.1 μ A during deep sleep	Not Listed	1 μ A	2 μ A	0.3 μ A
Peak Current	15 mA	3.3 mA	17 mA	50 mA	23 mA	20.5 mA

Maximum Packet size	20 b	Not Listed	Not Listed	100 b	Not Listed	Not Listed
Data rate	250 kbps, 1 Mbps, 2 Mbps	Not Listed	Not Listed	250 kbps	250 kbps	2 Mbps
Vin Range	1.8 V to 3.6 V	2 V to 3.6 V	2.3 V to 3.6 V	2.8 V to 3.4 V	2.4 V to 3.6 V	1.8 V to 3.6 V
Datasheet	Datasheet	Datasheet	"Datasheet"	Datashet	Datashet	Datasheet

4.5.3 Xbee S1 Analysis

Benchmark measurements showed that the Xbee S1 takes approximately 162 ms to transmit and consumes 45 mA. An appropriate output capacitance for transmission bursts can be found by [38]

$$C_{out} = (I \times t) / \Delta V \quad (12)$$

where ΔV is change in voltage, I is current, and t is time. Designing for an acceptable voltage drop of 1.5 V yields an output capacitance of 4860 μF . Equation (13) indicates that the output capacitor harvests 18.5 mJ of usable energy per transmission burst [23]. This calculation also provides an estimate for energy consumed by the transmission module during each cycle.

$$E_{harvest} = (C_{out} / 2) \times (V_{high}^2 - V_{low}^2) \quad (13)$$

The system transmits data every 62.4 s so the transmitter consumes 25.7 J per day. For most wireless sensor systems, radio transmissions are known to be the most power-hungry operation [61].

In its current setup, the MCU sends four bytes of data via the ZigBee transmitter during every transmission cycle. The first three bytes represent data collected from the analog temperature sensor (converted to temperature by the MCU) and the last byte represents the digital reading from the occupancy sensor. ZigBee packets are received and validated by a receiver connected to a PC where they are logged and plotted.

In a comprehensive microgrid system, this receiver would communicate with a controller designed to collect and analyze data from multiple sensors. The controller's primary function is to manage and switch discretionary loads on or off, enabling maximum energy savings. To guarantee reliability and prompt response to the data inputs, the system would likely be plugged in (connected to a constant power source) instead of relying on energy harvesting, alleviating the need for the extreme power efficiency crucial for the sensor node discussed in this paper.

Leveraging the ZigBee communication protocol enhances the system's ease of integration into existing microgrid setups that may already employ ZigBee technology. The transmitter's destination address can be easily changed to match the microgrid's receiver. This simple modification enables seamless communication and interoperability within the microgrid infrastructure.

4.6 System Power Budget

While the MCU and sensors can be powered from the LDO aboard the LTC3108, Fig. 12 illustrates the impact that additional loads have on the efficiency of the converter. To achieve maximum converter efficiency and to take advantage of the full sensitivity of the LTC3108, it makes sense to remove these loads and power them separately using a small coin-cell battery.

The MCU regularly enters LPM3 after each active cycle. At 3.3 V, the MCU consumes 369.2936 μA in active mode and 0.41 μA in LPM3 as measured by the SMU. The period of the cycle is 62.4 seconds as illustrated in Fig. 13. During each period the MCU is active for 400 ms. Using this information the duty cycle can be calculated.

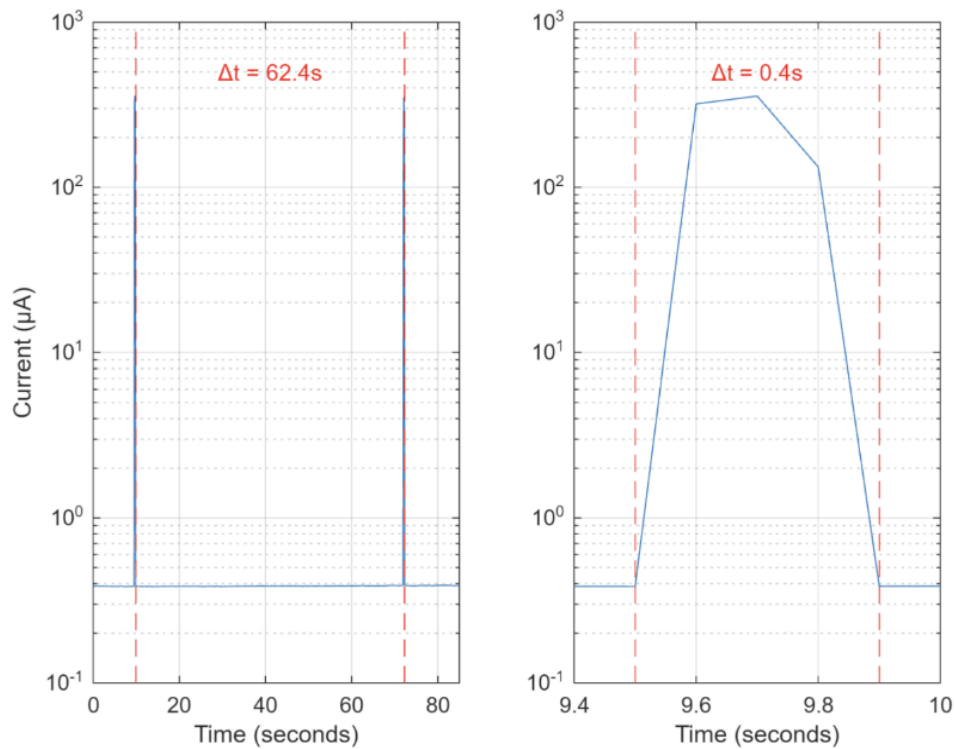


Fig. 13. MCU time between cycles (left) and active cycle time (right)

$$91.9s - 29.5s = 62.4s$$

$$Duty\ Cycle = \frac{0.4s}{62.4s} \times 100\% = 0.641\% \quad (14)$$

The digital subsystem exhibits a duty cycle of 0.641%, and the MCU consumes 0.2197 mWh or 0.791 J per day. A commonly available 3V coin cell battery, like the Panasonic CR2477, has a capacity of 1 Ah of energy. Using measured energy consumption data, calculations predict that a battery of this size could power the MCU for 37.4 years. The lifespan of coin-cell batteries is typically only 10 years. Given the longer-term savings enabled by this smart residential microgrid sensor, a decade of operation is an acceptable tradeoff for removing the MCU load from the harvester and freeing up harvesting potential.

In a 24-hour day, there are 86,400 seconds.

$$\frac{86400s}{62.4s} = 1384.615385 \text{ cycles per day}$$

$$Wh = power (W) \times time (h) \quad (15)$$

Active mode:

$$\begin{aligned} Power (W) &= Current (A) \times Voltage (V) = (369.2936)(10^{-6}) \times (3.3) \\ &= 0.0012186689 W \end{aligned}$$

$$Time (h) = ((553.846154 \text{ seconds}) / 60) / 60 = 0.1538461539 h$$

$$\begin{aligned} Energy (Wh) &= (0.0012186689 W) \times (0.1538461539 h) \\ &= (1.874875231)(10^{-4}) = 0.1874875231 mWh \end{aligned}$$

Passive mode:

$$Power (W) = (0.4100)(10^{-6}) \times (3.3) = (1.353)(10^{-6})W = 1.353 \mu W$$

$$Time (h) = ((85846.15387)/60)/60 = 23.84615385 h$$

$$\begin{aligned} Energy (Wh) &= ((1.353)(10^{-6}) W) \times (23.84615385 h) \\ &= (3.226384616)(10^{-5}) Wh = 0.0322638462 mWh \end{aligned}$$

$$Total Energy Consumption = 0.2197513693 mWh/day$$

After factoring the additional 1.694 J consumed by the sensor loads, the energy stored in a 1 Ah battery is enough to provide 11.9 years of operation with the operational duty cycle of 0.641%. If one were to add the 25.7 J of energy consumed daily by the transmitter to the battery's load, its life would be reduced to roughly 1 year. Removing the transmitter load from the battery and powering it using energy harvesting adds over 10 years to the system's lifespan, justifying the proposed hybrid design. This outcome is shown in Fig. 14, illustrating how the duty cycle can be adjusted to achieve the desired system battery life.

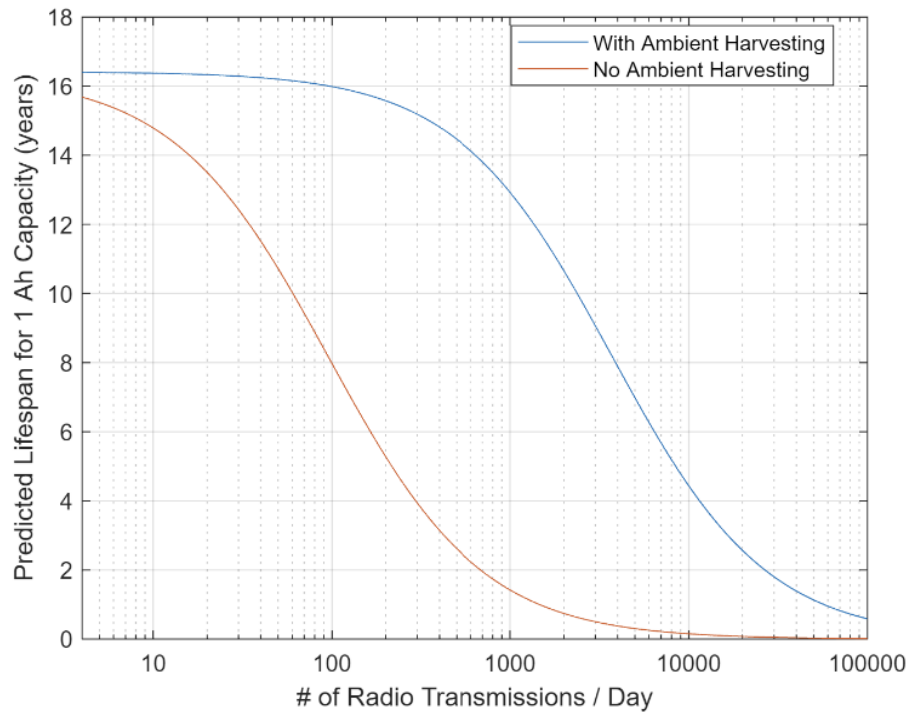


Fig. 14. Predicted lifespan for 1 Ah battery

Table 11 and Fig. 15 further illustrate the significance of removing the transmitter from battery power. By doing so, 90% of the energy that the system consumes is moved off the battery and powered with energy harvesting.

Table 11: Daily Energy Consumption of System Components

Component	Daily Energy Consumption
MSP430G2553 (MCU)	0.791 J
EKMB1103113 (PIR)	0.236 J
MCP9700A-E/TO (Temp)	1.46 J
Xbee S1 (Transmitter)	25.7 J

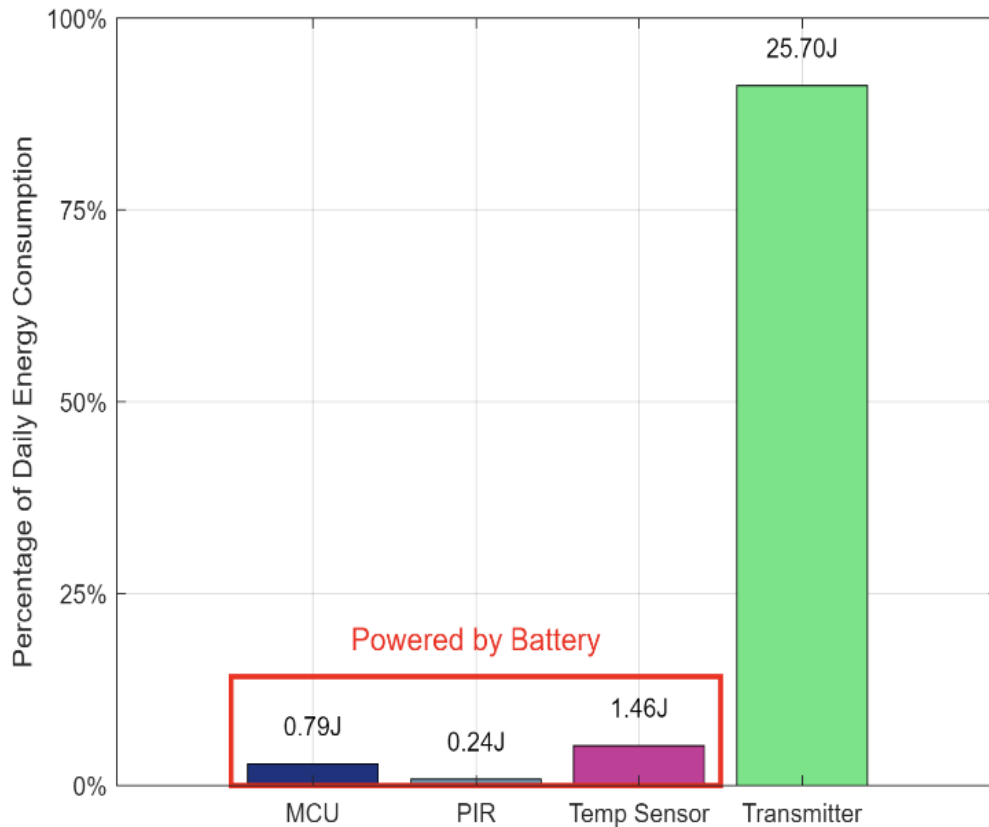


Fig. 15. System energy budget

4.6.1 Excess Energy Reservoir

When the 4860 μF output capacitor reaches full charge, any excess energy collected gets stored in the 1.5 F super-capacitor. The LTC3108 charges this capacitor to 5 V. When the ambient harvesting source becomes unavailable, the main output capacitor charges from the excess energy capacitor until its voltage drops below the regulated output. The 1.5 F capacitor provides 10.6 J of usable energy as its voltage drops from 5 V to 3.3 V. Based on voltage measurements, the output capacitor expends approximately

18.5 mJ of energy each transmission cycle, so the 1.5 F capacitor theoretically provides the sensor system with an additional 572 transmissions.

To test this calculation, a fully charged 1.5 F capacitor was connected to the storage pin of the LTC3108 and the MCU was configured to never enter sleep mode, allowing transmissions to occur immediately one after another. The storage element allowed the system to transmit 551 times which is close to (96% of) the calculated value.

Chapter 5: Data Collection and System Analysis

The following section details three main experiments designed to evaluate the robustness of the hybrid-system's operation and data transmission. The first experiment demonstrates that the harvesting sensor can be powered from a real transducer in real-world conditions. The second experiment focuses on the effect of a supercapacitor excess energy reservoir. The final experiment aims to reduce wasted energy and eliminate glitched transmissions.

5.1 Experiment 1

To prove that the system can operate with a real ambient energy source, the harvester was connected to a small 4.5 W monocrystalline PV cell mounted in a south-east-facing window in an indoor office room. The HVAC thermostat of the room was set to 22.22 °C. Additionally, temperature was only measured discretely at the nearest degree Fahrenheit. Occupancy data is not reported here as no one was present at the time of measurement. Data collection began just after noon and continued until the system

stopped transmitting at 5:00 PM when it could no longer collect sufficient solar energy to transmit. For this measurement, the 1.5 F storage capacitor was not connected, so the only energy available to the system was gathered from the PV cell. As sunset approached, the corresponding solar density lowered, and the harvester took longer to collect the energy required to transmit. This effect is shown in Fig. 16 by the data density that decreases during lower light hours.

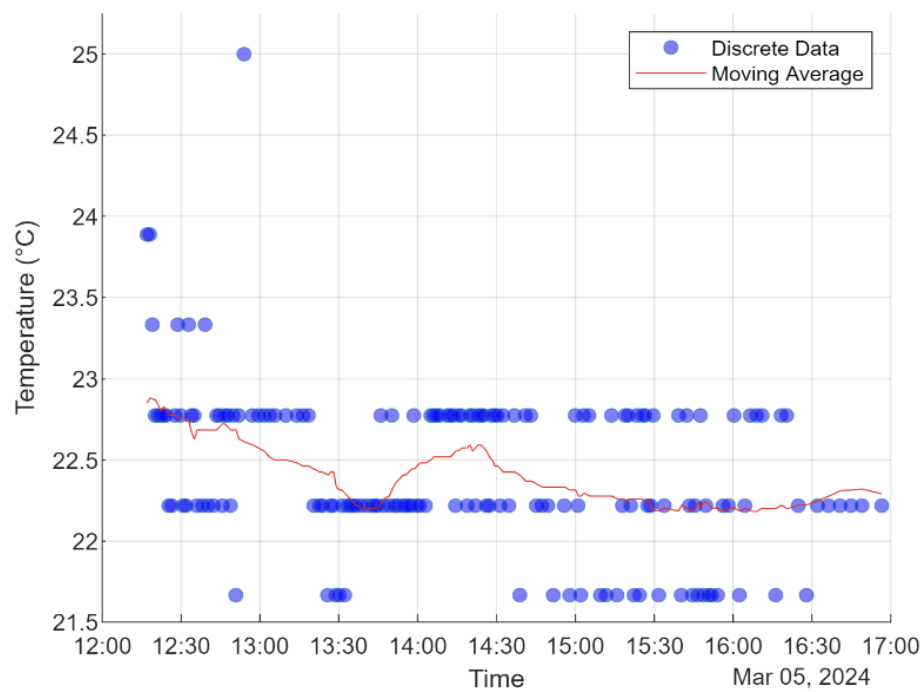


Fig. 16. Collected temperature data between 12:00 PM and 5:00 PM March 5

Fig. 16 illustrates that no additional information is gained by transmitting more frequently. Because no value is gained by the repeated transmission of identical data, it makes sense to adjust the data analysis system to transmit only when the data changes significantly, avoiding unnecessary transmissions and greatly reducing energy use.

In the 5-hour test described above and shown in Fig. 16, the system transmitted 165 times. If instead the system had only transmitted when the temperature changed by a full degree from the previous measurement, it would have transmitted 92 times. Eliminating 73 transmissions (44%) would result in 1.35 J of energy savings per day. This transmission threshold can be refined to save even more energy.

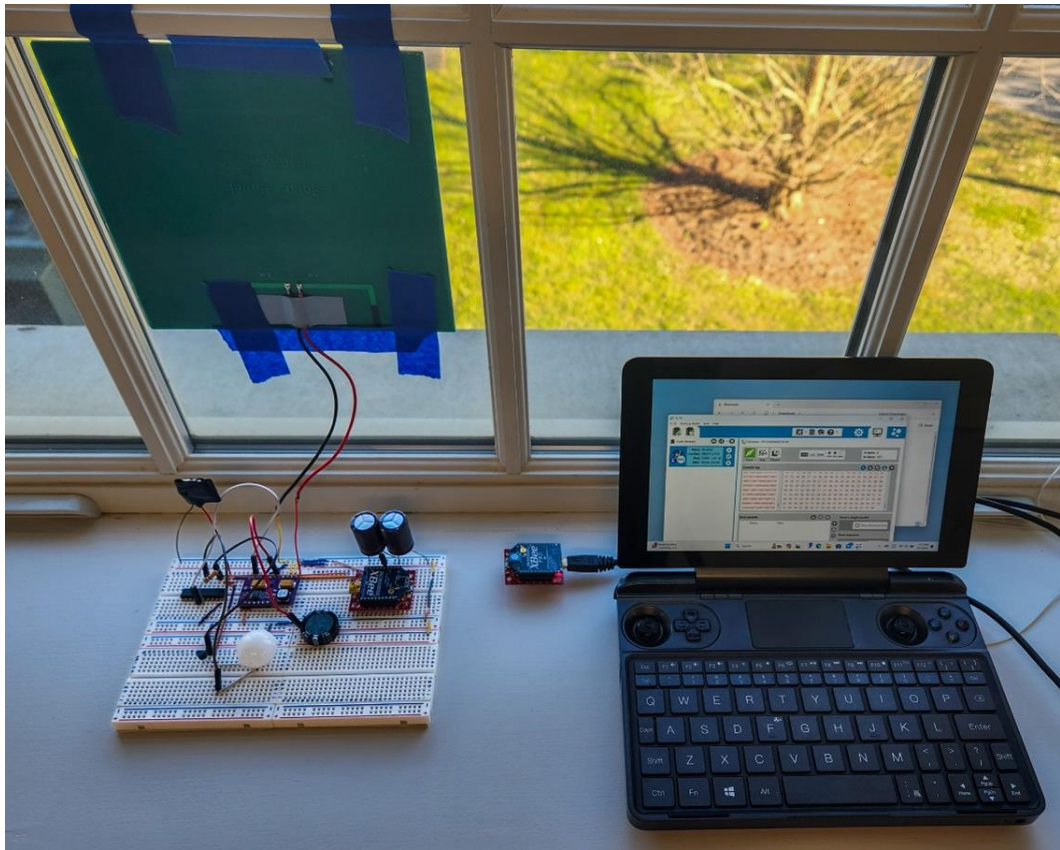


Fig. 17. Hybrid energy harvesting sensor experimental setup

5.2 Experiment 2

In the second series of experiments, the setup was placed in a south-east facing window for a period of several days and allowed to transmit with different super

capacitor storage elements. The first test was done using a 1.5 F super capacitor.

According to the math, this storage element, if fully charged, should allow for 572 operations after the harvesting source has disconnected or 9.6 hours of operating time into the night. In each of these experiments, the system is still programmed to transmit at the same duty cycle, every 62.4 seconds. In some cases, a transmission would get cut short resulting in a glitched transmission. For convenience, these have been removed from the following figures, however the nature of these glitched transmissions is explored later.

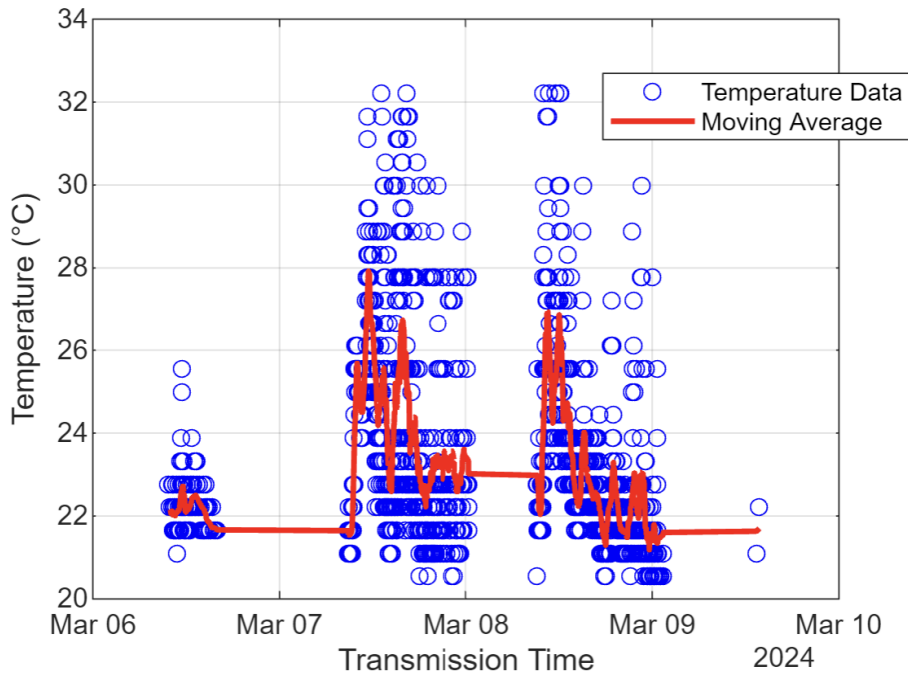


Fig. 18. Temperature data collected between March 6 and March 10 with a 1.5 F excess energy reservoir

The collected temperature data shows that the system was able to transmit well into the night, running out of energy a little after 12:00 PM. On March 8, the sun set at 6:07 PM and the system was able to transmit for roughly 6 hours beyond this, close to but under the calculated 9 hours.

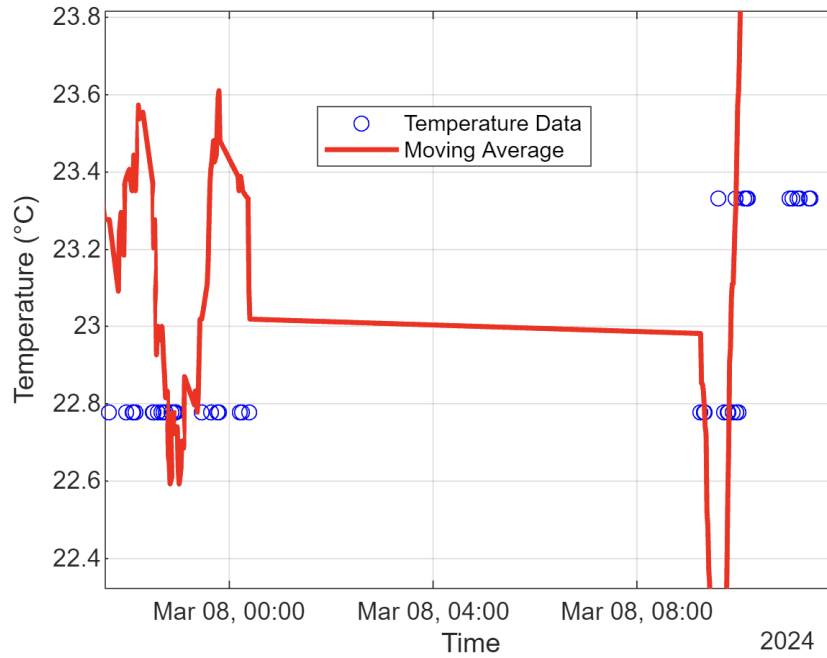


Fig. 19. Gap in transmission due to energy shortage

The system runs out of energy and does not transmit between the hours of 1:00 AM and 9:00 AM. This capacitor size is not sufficient for uninterrupted operation, but that is expected.

In the second experiment, the system was equipped with double the capacitance, 3 F. The experiment also took place over a larger number of days. With 3 F, the excess energy reservoir holds 21.1 J of usable energy, allowing for a theoretical 1145 transmissions or 18 hours of operation into the night. The data shows that the sensor

operates for significantly longer than in the previous experiment, although it still does fall short of continuous operation for brief periods late at night.

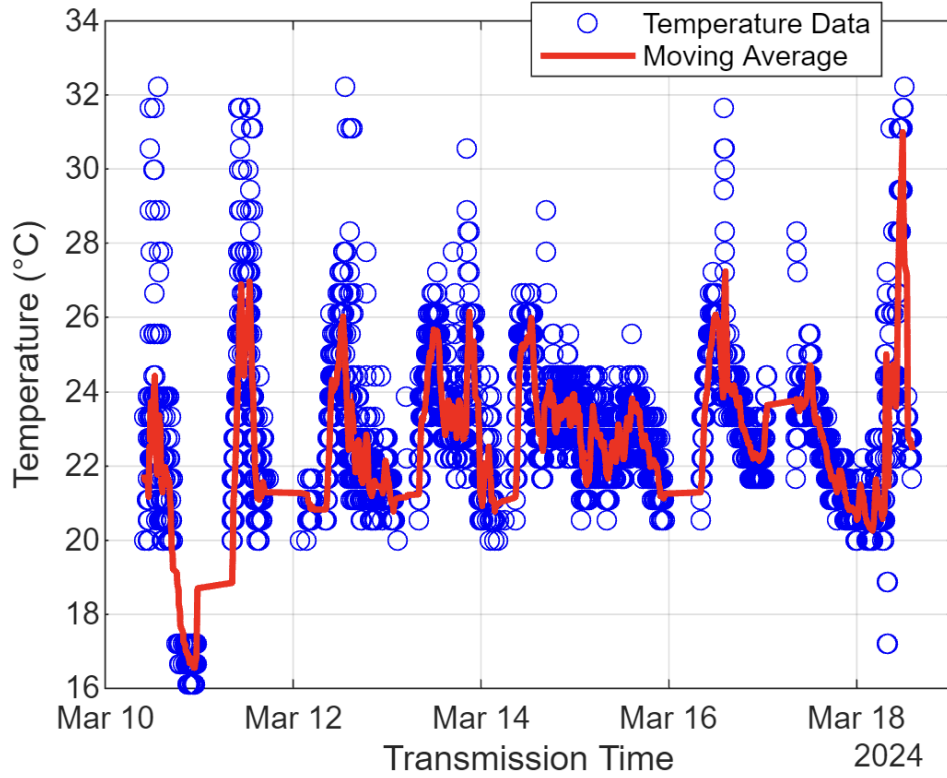


Fig. 20. Temperature data collected between March 10 and March 18 with a 3 F excess energy reservoir

Zooming in on a single day of operation reveals that even with a 3 F capacitance, there is a period between 4:00 AM and 9:00 AM where the system is inoperable or sends data very infrequently.

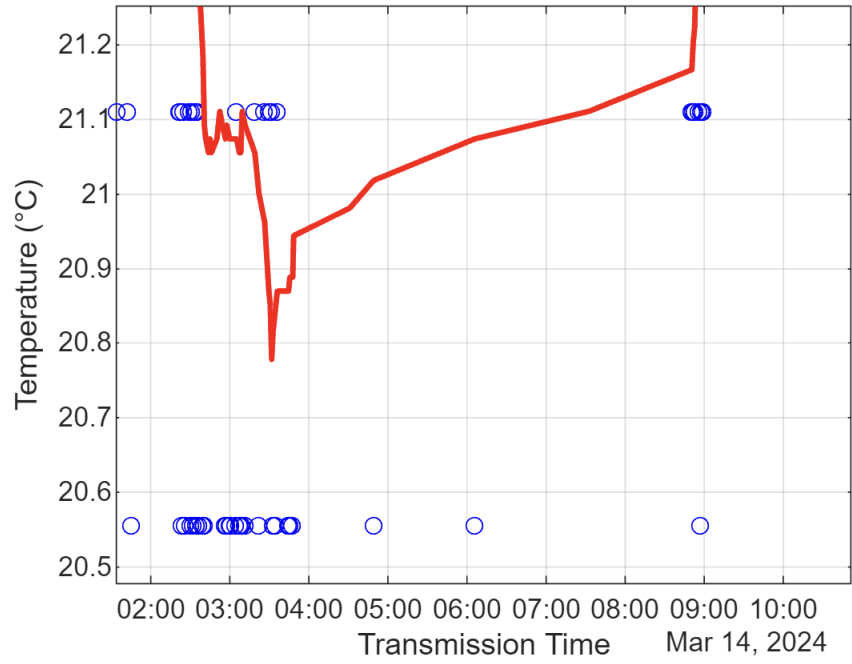


Fig. 21. Gap in transmission due to energy shortage

In the final experiment with this setup, the system was equipped with a 4.5 F capacitance for excess energy storage. Fig. 22 shows the collected temperature data.

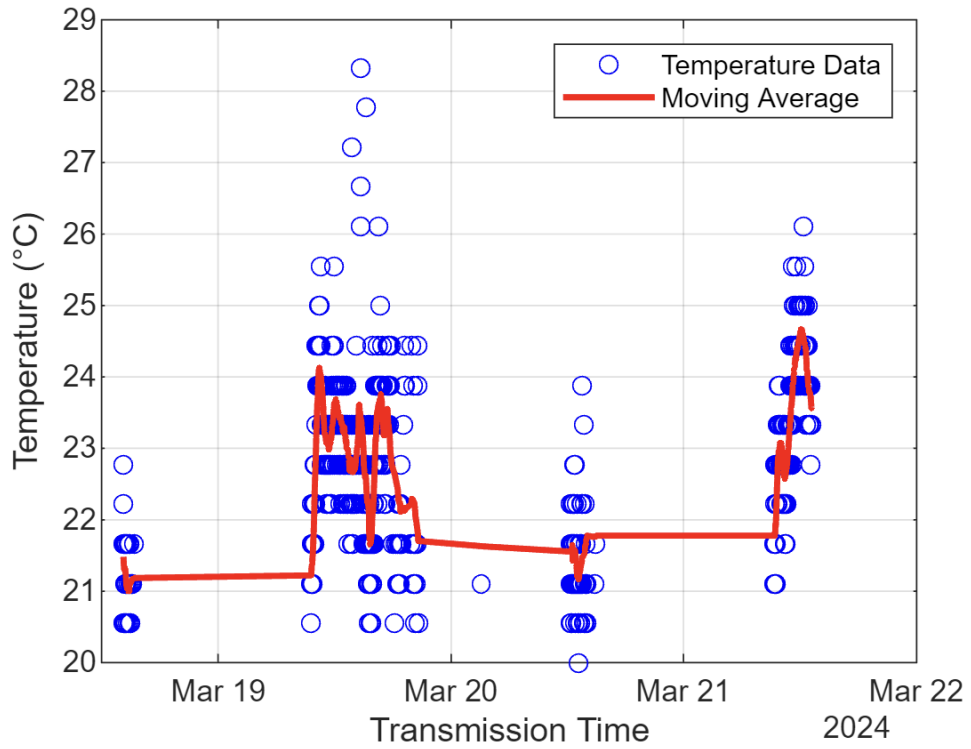


Fig. 22. Temperature data collected between March 19 and March 22 with a 4.5 F excess energy reservoir

This experiment was cut short due to unexpected results. The data seems to show that the system did not transmit for a significant portion of the day and night. In the previous data, transmissions that were cut short or did not send the correct data format were filtered from the figures. Looking at the data again with the glitched transmissions included reveals that the system was trying to transmit but was not sending complete messages. This factor also explains why the experiment with the 3 F supercapacitor appeared to stop transmitting short of a full day.

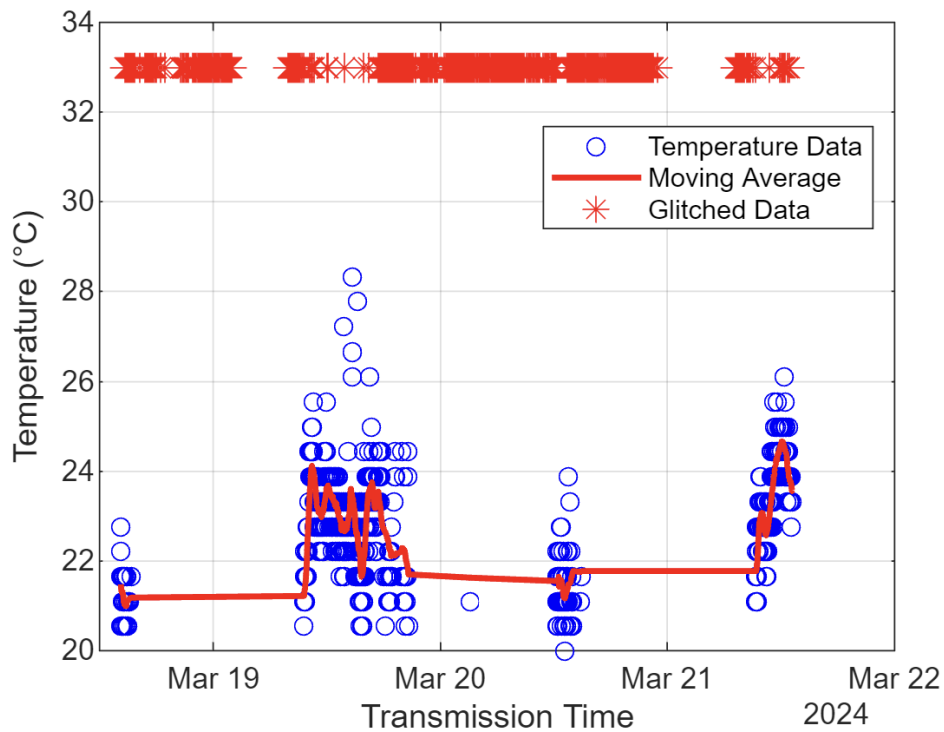


Fig. 23. Temperature data and glitched transmissions

In previous experiments, these glitched messages were significantly fewer and only occurred when the system had insufficient energy: early in the morning and late at night. However, in this case they start to present a serious issue. My theory was that the glitches were happening because the system had insufficient energy. The LTC3108 “power good” mosfet triggers when the output reaches 90% of its rated capacity. When the system is short on energy, it may attempt transmission before the capacitor reaches full charge. Supplying the RF transmitter with less energy than the system was designed for would result in a timing mismatch where the transmitter may not have enough time to transmit the entire message, resulting in gibberish read at the receiver. I theorized that extending the time in between transmissions would likely fix this issue.

5.3 Experiment 3

In this final experiment, the system was programmed to only transmit under specific circumstances: A) transmit if the temperature has changed by a full degree from the previously measured value, B) transmit if the occupancy sensor triggers an interrupt (with a cooldown to prevent continuous transmission attempts). This approach significantly reduced the energy consumption of the system and increased the average time between transmissions, so no glitched messages were transmitted.

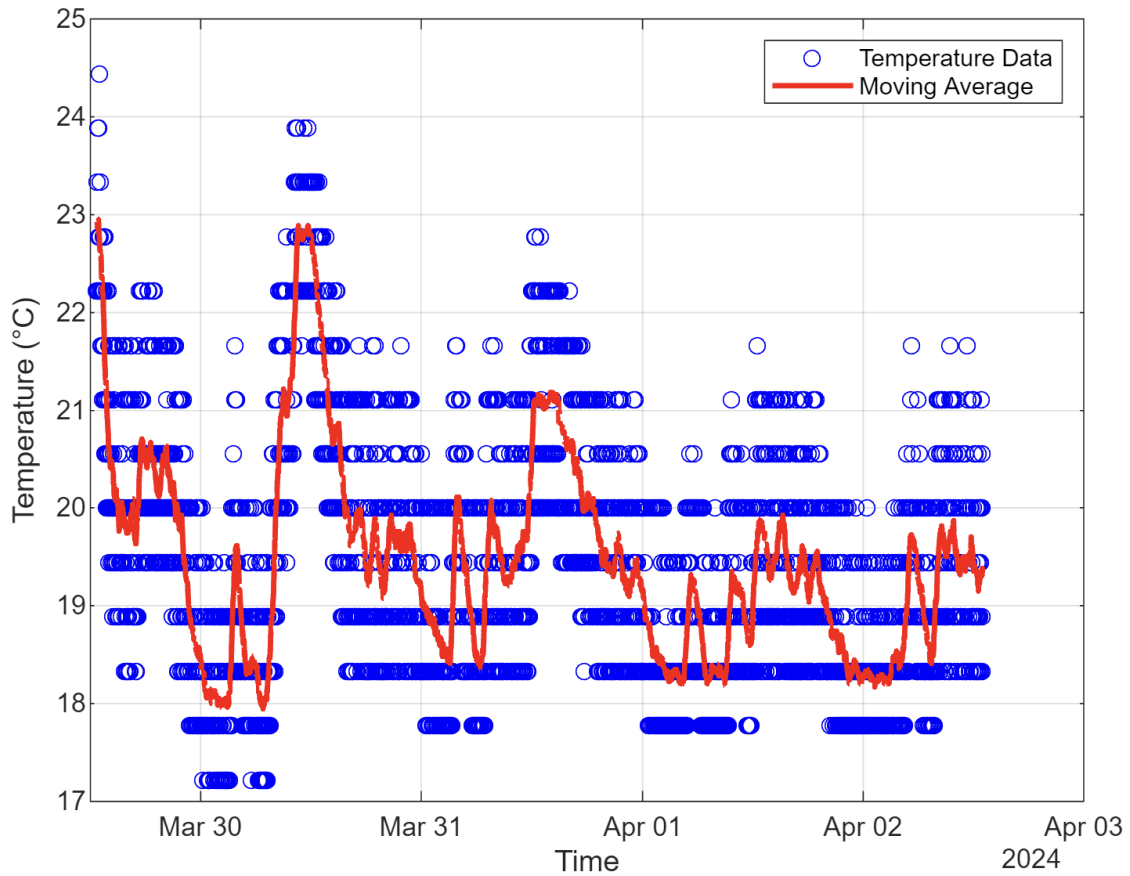


Fig. 24. Temperature data collected between March 29 and April 2 with data-aware program and a 4.5 F excess energy reservoir

Fig. 24 shows that the system transmitted for four days without interruption. Zooming into a single day illustrates this even better as seen in Fig. 25. On March 31, during the period between 12:00 PM and 5:00 PM, the same time period as experiment 1, the system transmitted data 201 times. If the system had transmitted with every MCU active cycle like in the first experiment, it would have transmitted 298 times. Adjusting the MCU code to only transmit when the temperature changes by a full degree resulted in 97 fewer transmissions (32%).

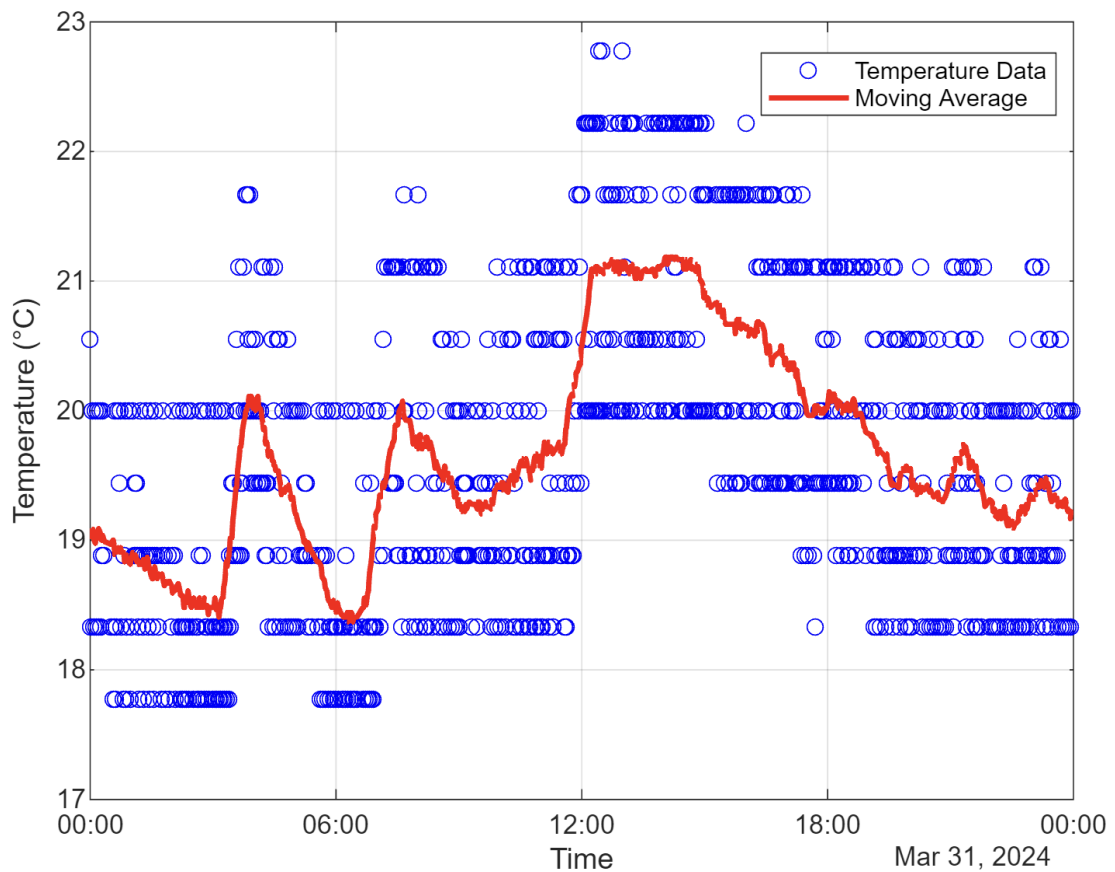


Fig. 25. Temperature data collected on March 31

The occupancy sensor can now interrupt the MCU's sleep mode and trigger a transmission as well, resulting in more accurate occupancy data as shown in Fig. 26. The data was taken in the Bucknell graduate student office, which does not get a lot of traffic, so the sparse occupancy detections make sense.

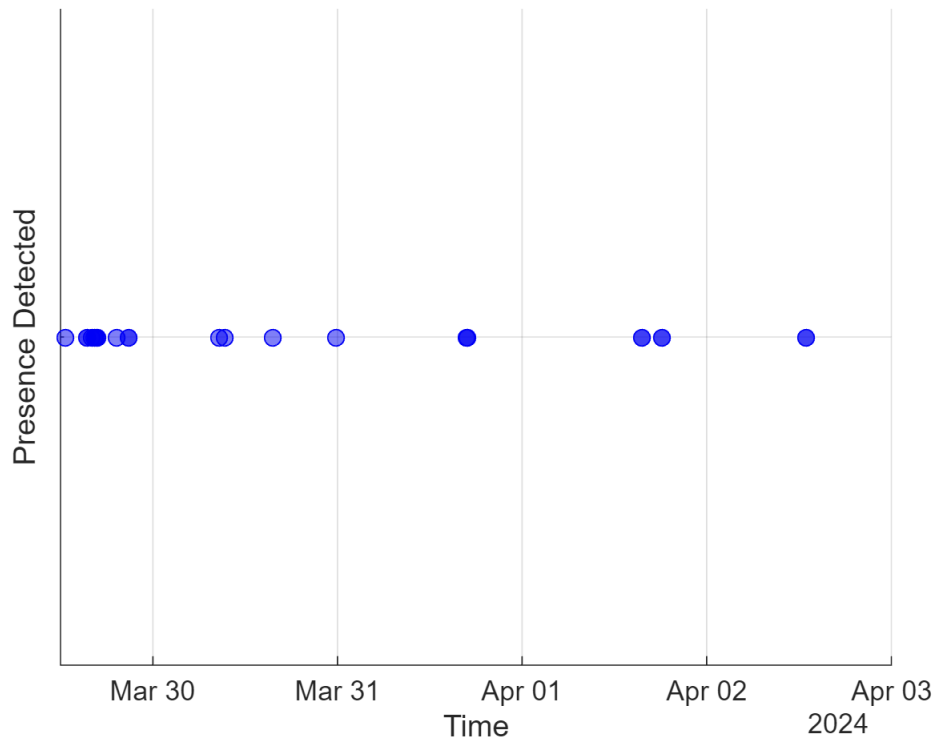


Fig. 26. Occupancy data collected between March 29 and April 2 with PIR interrupts

Reducing the excess energy reservoir capacitance to a lower 3 F value reveals that the system still achieves continuous operation with the new data-aware approach. Reducing it further to 1.5 F allows the system to run out of energy as in the second experiment. This confirms that 1.5 F is insufficient storage, even without transmission glitches. However, 3 F proves to be sufficient after eliminating glitched transmissions.

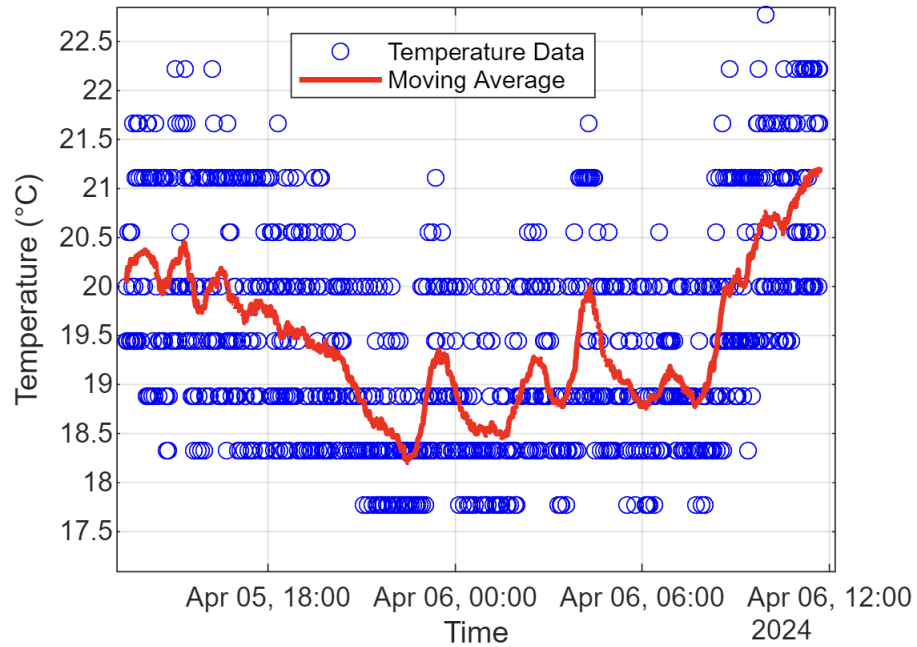


Fig. 27. Temperature data collected with data-aware approach and 3 F excess energy reservoir

Chapter 6: Conclusion

At the outset of this thesis, I delved into the existing research landscape surrounding microgrids, revealing a gap in the exploration of residential microgrids in contrast to their large-scale counterparts. My research bridges this gap by demonstrating the feasibility of employing energy harvesting to facilitate the deployment and extend the operating life of wireless sensor nodes within residential microgrid settings. I conducted a comprehensive evaluation of various energy harvesting sources, identifying PV cells and TEGs as offering the most utility due to their accessibility and the high energy densities they provide. A prototype hybrid battery and energy harvesting sensor was developed and evaluated, allowing energy harvesting from as little as $40 \mu\text{W}$.

6.1 Contributions to Knowledge

This thesis sought to address two fundamental inquiries: 1) identifying the ambient energy sources available in residential areas and determining which ones offer the highest energy density, and 2) assessing the viability of powering a microgrid sensor with energy harvesting. Through a thorough review of the literature and my empirical investigations, I highlighted the predominant ambient energy sources in residential settings. Solar and thermoelectric sources emerged as the most viable, characterized by their superior energy densities and availability.

6.1.1 Assessing the Viability of Powering a Microgrid Sensor with Energy Harvesting

My research and experimental findings confirmed the feasibility of using energy harvesting to power a microgrid sensor. However, I discovered that optimizing the use of environmental energy and maximizing the sensitivity of the harvesting IC can be more efficiently achieved by offloading smaller loads to battery power. This approach prioritizes the allocation of harvested energy for the more demanding RF transmitter, thus enhancing system efficiency.

In the prototype design segment, I outlined a modular system architecture through a block diagram, detailing potential components, the choices I made, and the rationale behind these decisions. This section simplifies the evaluation of each component's impact on the system's energy budget, providing a framework that allows for the easy substitution of components to tailor the system according to individual requirements.

Further, I examined the integration of a small coin cell battery and its impact on the system's longevity, illustrating the significant increase in system lifespan achieved by removing the RF transmitter from the battery source in favor of energy harvesting. This hybrid approach ensures that the system can operate continuously for over a decade without interruption.

I developed a microcontroller program to manage the duty cycle of MCU activity and data transmission efficiently. This program, enhanced to be both energy and data-aware, minimizes system energy consumption by initiating transmissions only when there is a change in data.

Lastly, I investigated the comparative energy storage capabilities of lithium-ion batteries versus supercapacitors within energy harvesting systems. My findings demonstrate that supercapacitors provide a robust energy storage solution, extending operational life by years without the need for battery replacements. Various capacitor sizes were tested to determine their ability to sustain sensor node operation post energy source depletion.

This thesis not only advances the understanding of energy harvesting applications within residential microgrids but also provides a practical guide for the development of efficient, long-lasting wireless sensor networks. Through a blend of theoretical insights and empirical evidence, it contributes significantly to the body of knowledge in the field, paving the way for future innovations in sustainable home energy management.

6.2 Lessons Learned

6.2.1 Timing

The primary issue I ran into while developing this system was incorrect timing between the MCU and transmitter. When the MCU detects that there is enough energy and decides to transmit, several things happen in quick succession. First, the MCU sets the gate of the LTC3108 MOSFET high, causing the output capacitor to connect and power the transmitter. Next, the MCU communicates the data to the RF transmitter via the UART protocol. The transmitter must then be awake and ready to receive this message, and then transmit this message to the receiver. To prevent the transmitter from continuing to pull current after transmission has ended, the MCU disconnects the transmitter from the output capacitor after sending the UART message. Within this sequence, there are several places where incorrect timing will prevent data transmission.

When the MCU triggers the MOSFET connecting the RF module to power, there is an inherent delay before the RF transmitter receives power. Additionally, the transmitter undergoes a brief initialization period during which it is incapable of receiving messages due to not being fully operational. Consequently, if the MCU transmits a UART message immediately after initiating power to the transmitter, the message is sent prematurely and fails to be acknowledged by the transmitter still in its startup phase. This timing can result in failed or glitched transmissions where partial data is sent and misinterpreted by the receiver. To address this issue, a brief delay is introduced prior to sending the message. However, modifications to the code can alter the timing required for the MCU to execute its operations, necessitating adjustments to this delay to ensure synchronicity with the transmitter's readiness.

Another timing challenge arises when the MCU disconnects the transmitter following a transmission. While it's advantageous to limit the duration that the transmitter is connected to the output capacitor to conserve energy, prematurely disconnecting the transmitter can lead to incomplete message transmission. This premature disconnection can cause transmission glitches or result in no data being transmitted at all.

The LTC3108 voltage regulator adds another layer of complexity to the system. This IC activates a "power good" signal once the capacitor's voltage reaches 90% of its full charge, which the MCU uses as a cue for initiating transmissions. When configured to supply 3.3 V, the "power good" signal is triggered as the output reaches just below 3 V. Setting the system's duty cycle too low may lead to attempts at transmission with only 3 V rather than the optimal 3.3 V. Although the capacitor may still hold enough energy, this reduced voltage can interfere with the timing which was configured for the higher voltage. The solution involves simply decreasing the duty cycle or extending the interval between transmissions to ensure the output capacitor reaches full charge. This discrepancy in timing is what led to glitches in some transmissions observed in experiment 2. Accordingly, adjusting the timing and decreasing the frequency of transmissions in experiment 3 successfully eliminated glitched transmissions.

6.2.2 UART Pulling Current

During the initial tests of the hybrid system, I observed a rapid decline in the coin cell battery voltage, which was surprising considering the sensors and MCU were expected to consume around 10 μ A. However, current measurements showed the battery

was discharging at nearly 3mA, leading to the voltage drop. Further examination pinpointed the MCU's UART pin as the issue.

Although the transmitter was powered off between transmissions, it remained connected to ground. The MSP430's UART pin is set high by default when not transmitting, allowing the transmitter to inadvertently draw 3mA of current through the UART pin. The resolution involved altering the code to set the UART pin to GPIO low when not actively transmitting. Additionally, a Schottky diode was introduced between the MCU's UART pin and the transmitter, effectively blocking any undesired current flow into the transmitter.

6.2.3 Sensor Accuracy

The original design of the system enabled all components to be powered via energy harvesting, leveraging the 2.2 V Low Dropout Regulator (LDO) on the LTC3108 for the sensors and MCU, providing a stable and regulated voltage. However, shifting these smaller loads to a small coin cell battery significantly enhanced the system's energy harvesting capacity. Using direct battery power for certain sensors can introduce error. The digital nature of the occupancy sensor means it remains unaffected by this change. In contrast, the analog temperature sensor used in the prototype outputs a voltage proportional to its power source. As the battery's voltage declines over time, the temperature readings interpreted by the MCU will incrementally increase. This variance might be negligible for most of the sensor's operational life, but as the coin cell battery depletes, temperature measurements could become skewed. One solution is to implement a simple voltage regulator between the battery and the temperature sensor to stabilize the power supply, although this adds another component's energy usage into the equation.

Alternatively, employing the temperature sensor integrated into the MCU could circumvent these issues.

After some further testing, the MSP430 internal temperature sensor faces similar issues. The analog reading from the internal temperature sensor is also dependent on the voltage powering the MCU. The MSP430 can use an internal 2.5 V reference voltage for ADC calculations, but further calibration of the sensor is required to obtain accurate readings.

Chapter 7: Next Steps

7.1 Cost Analysis

Something established in the background section is that energy harvesting sensors should be low-cost, have low-cost operation, and enable continuous sensing. This thesis thoroughly explored how an energy harvesting sensor could reduce microgrid maintenance by mitigating reliance on battery technology. It also explored techniques for minimizing energy usage, with the final design allowing uninterrupted sensing. A potential area for further investigation is the actual cost of the sensors. The components chosen for the prototype design were chosen based on compatibility, ease of use, and getting the maximum value out of the simplest design. The price of individual components was not considered.

Table 12: Component Prices

Component	Price
LTC3108 IC	\$10
MSP430G2553	\$2.9
Xbee Transmitter	\$29.33
EKMB1103113 PIR Sensor	\$25.35
MCP9700A-E/TO Temperature Sensor	\$0.61
2200 μ F Capacitor (x2)	\$1.7
4.5 F Capacitor	\$2.42
4.5 W Monocrystalline PV Cell	\$15.99
Total	\$88.3

The main source of cost in the system is the Xbee transmitter and the PIR sensor. The cost of the system could be minimized with further research and component analysis.

7.2 Integration With Residential Microgrid

This thesis has explored the effectiveness of a hybrid energy-harvesting and battery-powered sensor at providing robust and maintenance-free communication, facilitating the integration of sensors into microgrid systems. The research primarily concentrates on developing and assessing the sensor's performance. The next phase involves incorporating the sensor into an operating residential microgrid system. Integrating one or more hybrid sensors into a microgrid could offer insights into how these sensors affect the complexity of integration and whether they save time and effort during installation compared to conventional sensors. Future work could investigate the

optimal placement of sensors in a residential microgrid to maximize ambient energy. Additionally, real world energy savings achieved can be measured against the projected savings proposed in this study. To enhance the system's effectiveness, reevaluating the accuracy and calibration of the temperature sensor is crucial to ensure that the microgrid receives accurate environmental data.

7.3 Energy Harvesting Standard

In the process of designing an energy-harvesting sensor system, a principal focus has been on the ease of integration and use. Prior to the experimental phase, it was essential to validate the concept of an energy-harvesting sensor not merely through theoretical speculation but via mathematical justification. This approach led to a detailed examination of component datasheets; a task complicated by the lack of a standardized format across manufacturers. It became apparent that while two devices might fulfill similar roles, their datasheets could present vastly different information, sometimes omitting critical comparative metrics altogether.

7.3.1 Challenges in Component Selection:

The exploration of communication modules revealed consistent provision of data on peak and sleep currents, along with voltage range. Yet other potentially important details such as maximum packet size, maximum consecutive transmission time, peak current duration, and even data rate were frequently missing. This inconsistency poses a significant obstacle in selecting the most energy-efficient components for the system.

Compatibility concerns further complicate the selection process. An example is the MRF24J40MA-I/RM RF module from Microchip Technology, which, despite its low power consumption, is optimized for integration with PIC microcontrollers. Its reliance on a specific communication protocol (4-wire SPI) and limited documentation for interfacing with non-PIC MCUs illustrate the potential lock-in effect, where choosing a particular component can constrain the overall system to a singular development environment.

Moreover, the appeal of many transmitter modules that advertise minimal current draw is tempered by the fact that many incorporate embedded MCUs. This feature might streamline certain aspects of system development, depending on the designer's skills and the project's requirements, but it also restricts the development process to the proprietary environment of the module.

7.3.2 Towards a Standardized Framework:

A standardized framework for RF transmitter modules would clearly delineate essential specifications such as the minimum RF range or transmission distance, tailored to the nuances of residential environments. It would detail the necessary transmission speed and active duration for RF modules, accounting for any startup times to ensure successful data transmission.

For sensors, the standard would encompass not just current consumption figures but also specify the communication protocol, distinguishing between digital and analog methods to facilitate accurate system design and integration.

In the realm of energy harvesting ICs, a uniform standard would include specifications on output current, efficiency and power metrics, and the minimum operational power, offering a comprehensive overview to guide optimal component selection.

My journey through researching and designing an energy-harvesting sensor system has underscored the critical need for a standardized approach to component specification and selection. Such a standard would not only clarify performance metrics and operational requirements but also address compatibility issues, significantly simplifying the design process. By establishing clear benchmarks and guidelines, it would pave the way for future advancements in energy-harvesting technology, enabling engineers to push the boundaries of what is possible in creating sustainable, efficient sensor networks for residential microgrid and beyond.

Appendix 1.

MSP430G2553 Code

```
#include <msp430.h>

volatile unsigned int wakeUpSource = 0; // Global flag to indicate wake-up
source: 0 for timer, 1 for PIR
volatile unsigned int okToTransmit = 1; // Flag to let the main loop know it
is OK to transmit
volatile unsigned int adcReady = 0; // Flag to indicate when ADC reading is
ready

UART_Init()
{
    P1SEL |= BIT2;        // P1.2 = TXD
    P1SEL2 |= BIT2;
    UCA0CTL1 |= UCSSEL_2; // SMCLK
    UCA0BR0 = 104;        // 1MHz 9600
    UCA0BR1 = 0;
    UCA0MCTL = UCBR50;    // Modulation UCBR5x = 1
    UCA0CTL1 &= ~UCSWRST; // **Initialize USCI state machine**
}

UART_SendChar(char data)
{
    (!(IFG2 & UCA0TXIFG)); // USCI_A0 TX buffer ready?
    UCA0TXBUF = data;      // TX -> RXed character
}

configureUnusedPorts()
{
    // Initialize unused pins on Port 2
    P2OUT = 0x00; // Set all pins on Port 2 to low
    P2DIR = 0xFF; // Set all pins on Port 2 as outputs

    // Initialize unused pins on Port 3
    P3OUT = 0x00; // Set all pins on Port 3 to low
    P3DIR = 0xFF; // Set all pins on Port 3 as outputs
}

void initADC();
void initLowPowerMode();
void initGPIO();
void initTimer();

volatile int adcResult; // Declare a volatile variable to store ADC result
// this is the status of the Power Good pin from the LTC3108
volatile int adcResult2;
// this is the sensor value
```

```

volatile int temperature;
int lastTemperature = -1; // Last measured temperature, initialized to an
impossible value

int main(void)
{
    WDTCTL = WDTPW + WDTHOLD; // Stop the watchdog timer
    configureUnusedPorts();

    // Configure P1.0 and P1.1 as analog inputs
    P1SEL |= BIT0 + BIT1;
    P1SEL2 |= BIT0 + BIT1;

    // Configure ADC10
    ADC10CTL1 = INCH_0; // Select channel A0 (P1.0)
    ADC10CTL0 = SREF_0 + ADC10SHT_3 + ADC10ON + ENC; // Set reference voltage,
ADC10 on, enable conversion

    initLowPowerMode();
    initGPIO();
    initTimer();
    UART_Init(); // Initialize UART

    __enable_interrupt(); // Enable global interrupts

    while (1)
    {
        ADC10CTL0 &= ~ENC; // Disable ADC to configure
        ADC10CTL1 = INCH_0; // Select channel A0 (P1.0)
        ADC10CTL0 = SREF_0 + ADC10SHT_3 + ADC10ON + ENC; // Configure and
enable ADC
        delay_cycles(20000); // Add a delay

        // Start conversion for ADC channel A0 (P1.0)
        ADC10CTL0 |= ADC10SC;
        // Wait for conversion to complete
        while (ADC10CTL1 & ADC10BUSY);
        // Store result in adc_value1
        adcResult = ADC10MEM;

        P1SEL |= BIT2; // P1.2 = TXD
        P1SEL2 |= BIT2; // P1.2 = TXD

        // Reset ADC10
        ADC10CTL0 &= ~ENC;
        // Configure ADC10 for channel A1 (P1.1)
        ADC10CTL1 = INCH_1;
        delay_cycles(20000);
        // Start conversion for ADC channel A1 (P1.1)
        ADC10CTL0 |= ENC + ADC10SC;
        // Wait for conversion to complete
        while (ADC10CTL1 & ADC10BUSY);
        // Store result in adc_value2
    }
}

```

```

adcResult2 = ADC10MEM;

// Convert to temperature
temperature = (((((float)adcResult2/1024)*3.0)-
0.5)/.01)*((float)9/5)+32;

// Reset ADC10
ADC10CTL0 &= ~ENC;

int tempInt = (int)temperature; // Convert temperature to an integer

// Always read PIR sensor state and send its value
int digitalInput = (P1IN & BIT4) ? 1 : 0;

// Transmission logic

if (wakeUpSource == 1 && adcResult > 350) // If woken by PIR
{
    if (okToTransmit == 1) {

        P1OUT |= BIT7;
        delay_cycles(30000);

        // Always send temperature and PIR state
        UART_SendChar((char)(tempInt / 100) + '0'); // Hundreds
        UART_SendChar((char)((tempInt % 100) / 10) + '0'); // Tens
        UART_SendChar((char)(tempInt % 10) + '0'); // Ones
        UART_SendChar(digitalInput + '0'); // PIR state
        lastTemperature = tempInt; // Update last known temperature
        okToTransmit = 0;

    }
}
else if (wakeUpSource == 0 && adcResult > 350) // If woken by Timer
{

    okToTransmit = 1;
    // Only send if temperature has changed by at least 1 degree

    if (lastTemperature == -1 || (lastTemperature - tempInt) >= 1)
    {
        P1OUT |= BIT7;
        delay_cycles(30000);

        UART_SendChar((char)(tempInt / 100) + '0'); // Hundreds
        UART_SendChar((char)((tempInt % 100) / 10) + '0'); // Tens
        UART_SendChar((char)(tempInt % 10) + '0'); // Ones
        UART_SendChar(digitalInput + '0'); // PIR state
        lastTemperature = tempInt; // Update last known temperature

    }
}
}

```

```

        // Reset wake-up source to ensure correct behavior on next loop
iteration
        wakeUpSource = 0; // Reset to default (timer)

        delay_cycles(100000);
        P1OUT &= ~BIT7;

        P1SEL &= ~BIT2; // Clear P1.2 function select to general I/O
        P1SEL2 &= ~BIT2; // Clear P1.2 function select to general I/O
        P1DIR |= BIT2; // Set P1.2 as output
        P1OUT &= ~BIT2; // Set P1.2 to low

        // Disabling PIR interrupt
        (okToTransmit == 0) {
            P1IE &= ~BIT4; // Disable PIR interrupt by clearing interrupt
enable for P1.4
        }

        // Enabling PIR interrupt
        (okToTransmit == 1) {
            P1IE |= BIT4; // Enable PIR interrupt by setting interrupt enable
for P1.4
        }

        __bis_SR_register(LPM3_bits + GIE); //Enter LPM3

    }

    //return 0;
}

    initADC()
{
    ADC10CTL1 |= ADC10DIV_3; // Set the ADC clock divider
    ADC10CTL0 = SREF_0 + ADC10SHT_3 + ADC10ON + ADC10IE; // Vr+ = AVcc and Vr-
= AVss, ADC ON, ADC sampling time, enable ADC interrupt
}

    initLowPowerMode()
{
    BCSCTL1 = CALBC1_1MHZ; // Set DCO to 1MHz
    DCOCTL = CALDCO_1MHZ;

    BCSCTL3 |= LFXT1S_2; // Set ACLK to VLO

    __bis_SR_register(SCG0); // Disable the FLL control loop
    BCSCTL1 |= DIVA_3; // Divide ACLK by 8
    __bic_SR_register(SCG0); // Enable the FLL control loop
}

    initGPIO()
{
    P1DIR |= BIT6; // Set P1.6 as an output
    P1DIR |= BIT7; // Set P1.7 as an output
}

```

```

    P1OUT &= ~BIT7;           // Initialize P1.7 to low
    P1DIR &= ~BIT4;         // Set P1.4 as input
    P1REN |= BIT4;          // Enable pull-up/pull-down
resistor
    P1OUT &= ~BIT4;         // Set pull-down resistor (input
low by default)

    // Configure P1.4 for interrupt
    P1IE |= BIT4; // Enable interrupt for P1.4
    P1IES &= ~BIT4; // Trigger on rising edge
    P1IFG &= ~BIT4; // Clear interrupt flag for P1.4
}

// PORT1 Interrupt Service Routine for PIR sensor
vector=PORT1_VECTOR
__interrupt void Port_1(void) {
    (P1IFG & BIT4) { // Check P1.4 interrupt
        wakeUpSource = 1; // Set wake-up source to PIR
        __bic_SR_register_on_exit(LPM3_bits); // Exit LPM3
        P1IFG &= ~BIT4; // Clear interrupt flag for P1.4
    }
}

    initTimer()
{
    CCTL0 = CCIE;           // Enable interrupt for CCR0
    TACTL = TASSEL_1 + ID_3 + MC_1; // ACLK, divide by 8, up mode
    CCR0 = 12500;           // Set CCR0 to generate interrupt
every 1 second
}

// Timer A0 interrupt service routine
vector=TIMER0_A0_VECTOR
__interrupt void Timer_A(void)
{
    wakeUpSource = 0; // Set wake-up source to timer
    __bic_SR_register_on_exit(CPUOFF); // Wake up the CPU
}

// ADC10 interrupt service routine
vector=ADC10_VECTOR
__interrupt void ADC10_ISR(void)
{
    __bic_SR_register_on_exit(CPUOFF); // Clear CPUOFF bit from 0(SR)
}

```


References

- [1] P. Diefenderfer, P. M. Jansson, and E. R. Prescott, "Application of power sensors in the control and monitoring of a residential microgrid," in *2015 IEEE Sensors Applications Symposium (SAS)*, Apr. 2015, pp. 1–6. doi: 10.1109/SAS.2015.7133612.
- [2] M. Kabalan *et al.*, "Commissioning a Real-World Industry-Grade Microgrid with Undergraduate and Graduate Students: An Educational Experience," in *2021 North American Power Symposium (NAPS)*, Nov. 2021, pp. 1–6. doi: 10.1109/NAPS52732.2021.9654730.
- [3] F. J. Bellido Outeirino, J. F. Arias, M. Linan-Reyes, and E. Palacios-Garcia, "In-home power management system based on WSN," in *2013 IEEE International Conference on Consumer Electronics (ICCE)*, Las Vegas, NV: IEEE, Jan. 2013, pp. 546–547. doi: 10.1109/ICCE.2013.6487013.
- [4] A. Safdarian, M. Fotuhi-Firuzabad, and M. Lehtonen, "Optimal Residential Load Management in Smart Grids: A Decentralized Framework," *IEEE Transactions on Smart Grid*, vol. 7, no. 4, pp. 1836–1845, Jul. 2016, doi: 10.1109/TSG.2015.2459753.
- [5] M. Erol-Kantarci and H. T. Mouftah, "Wireless Sensor Networks for Cost-Efficient Residential Energy Management in the Smart Grid," *IEEE Transactions on Smart Grid*, vol. 2, no. 2, pp. 314–325, Jun. 2011, doi: 10.1109/TSG.2011.2114678.
- [6] S. Damodaran and B. Sridharan, "PIR Sensor Based Motion Detection using Fuzzy Controller," vol. 8, no. 1, 2019.

- [7] S. Verma and P. Rana, “Wireless communication application in smart grid: An overview,” in *2014 Innovative Applications of Computational Intelligence on Power, Energy and Controls with their impact on Humanity (CIPECH)*, Nov. 2014, pp. 310–314. doi: 10.1109/CIPECH.2014.7019038.
- [8] V. Gungor, B. Lu, and G. Hancke, “Opportunities and Challenges of Wireless Sensor Networks in Smart Grid,” *Industrial Electronics, IEEE Transactions on*, vol. 57, pp. 3557–3564, Nov. 2010, doi: 10.1109/TIE.2009.2039455.
- [9] M. Krishnasamy, J. R. Shinde, H. P. Mohammad, U. Deepesh, and T. R. Lenka, “Design and Simulation of Smart Flooring Tiles using Two-Phased Triangular Bimorph Piezoelectric Energy Harvester,” in *2020 IEEE-HYDCON*, Sep. 2020, pp. 1–4. doi: 10.1109/HYDCON48903.2020.9242839.
- [10] J. Lippelt and M. Sindram, “Global Energy Consumption,” *CESifo Forum*, vol. 12, pp. 80–82, Jan. 2011.
- [11] W. Lutz, W. Butz, and K. Samir, *World Population & Human Capital in the Twenty-First Century: An Overview*. Oxford University Press, 2017.
- [12] “U.S. energy consumption increases between 0% and 15% by 2050.” Accessed: Dec. 05, 2023. [Online]. Available: <https://www.eia.gov/todayinenergy/detail.php?id=56040>
- [13] A. M. Elhalwagy, M. Y. M. Ghoneem, and M. Elhadidi, “Feasibility Study for Using Piezoelectric Energy Harvesting Floor in Buildings’ Interior Spaces,” *Energy Procedia*, vol. 115, pp. 114–126, Jun. 2017, doi: 10.1016/j.egypro.2017.05.012.

- [14] H. Talei, B. Zizi, M. R. Abid, M. Essaïdi, D. Benhaddou, and N. Khalil, "Smart campus microgrid: Advantages and the main architectural components," in *2015 3rd International Renewable and Sustainable Energy Conference (IRSEC)*, Dec. 2015, pp. 1–7. doi: 10.1109/IRSEC.2015.7455093.
- [15] A. Safdarian, M. Fotuhi-Firuzabad, and M. Lehtonen, "Benefits of Demand Response on Operation of Distribution Networks: A Case Study," *IEEE Systems Journal*, vol. 10, no. 1, pp. 189–197, Mar. 2016, doi: 10.1109/JSYST.2013.2297792.
- [16] "DOE_Benefits_of_Demand_Response_in_Electricity_Markets_and_Recommendations_for_Achieving_Them_Report_to_Congress.pdf." Accessed: Mar. 29, 2024. [Online]. Available: https://www.energy.gov/sites/default/files/oeprod/DocumentsandMedia/DOE_Benefits_of_Demand_Response_in_Electricity_Markets_and_Recommendations_for_Achieving_Them_Report_to_Congress.pdf
- [17] J. [R-T.-6 Rep. Barton, "H.R.6 - 109th Congress (2005-2006): Energy Policy Act of 2005." Accessed: Mar. 29, 2024. [Online]. Available: <https://www.congress.gov/bill/109th-congress/house-bill/6>
- [18] Y. Yang, D. Divan, R. G. Harley, and T. G. Habetler, "Power line sensornet - a new concept for power grid monitoring," in *2006 IEEE Power Engineering Society General Meeting*, Jun. 2006, p. 8 pp.-. doi: 10.1109/PES.2006.1709566.
- [19] F. M. Cruz, A. E. Molero, E. Castillo, M. Becherer, A. Rivadeneyra, and D. P. Morales, "Why Use RF Energy Harvesting in Smart Grids," in *2018 IEEE 23rd International Workshop on Computer Aided Modeling and Design of Communication*

Links and Networks (CAMAD), Barcelona, Spain: IEEE, Sep. 2018, pp. 1–6. doi:
10.1109/CAMAD.2018.8514966.

[20] M. Kabalan, P. Singh, and M. Moncada, “Assessment of potential microgrid system comprising renewable energy in La Kasqita Community, Nicaragua,” May 2015, pp. 1–5. doi: 10.1109/IHTC.2015.7238067.

[21] H. Irie, K. Hirose, T. Shimakage, and J. Reilly, “The Sendai Microgrid Operational Experience in the Aftermath of the Tohoku Earthquake: A Case Study,” Mar. 2013.

[22] A. Hajizadeh, M. Soltani, and L. E. Norum, “Intelligent power control of DC microgrid,” in *2017 IEEE 17th International Conference on Ubiquitous Wireless Broadband (ICUWB)*, Sep. 2017, pp. 1–5. doi: 10.1109/ICUWB.2017.8251006.

[23] M. Honda, T. Sakurai, and M. Takamiya, “Wireless temperature and illuminance sensor nodes with energy harvesting from insulating cover of power cords for building energy management system,” in *2015 IEEE PES Asia-Pacific Power and Energy Engineering Conference (APPEEC)*, Nov. 2015, pp. 1–5. doi:
10.1109/APPEEC.2015.7381080.

[24] V. C. Gungor and F. Lambert, “A Survey on Communication Networks for Electric System Automation,” *Computer Networks*, vol. 50, pp. 877–897, May 2006, doi: 10.1016/j.comnet.2006.01.005.

[25] V. C. Gungor and G. P. Hancke, “Industrial Wireless Sensor Networks: Challenges, Design Principles, and Technical Approaches,” *IEEE Transactions on*

Industrial Electronics, vol. 56, no. 10, pp. 4258–4265, Oct. 2009, doi:
10.1109/TIE.2009.2015754.

[26] B. Lu and V. C. Gungor, “Online and Remote Motor Energy Monitoring and Fault Diagnostics Using Wireless Sensor Networks,” *IEEE Transactions on Industrial Electronics*, vol. 56, no. 11, pp. 4651–4659, Nov. 2009, doi: 10.1109/TIE.2009.2028349.

[27] Y. Yang, F. Lambert, and D. Divan, “A Survey on Technologies for Implementing Sensor Networks for Power Delivery Systems,” in *2007 IEEE Power Engineering Society General Meeting*, Jun. 2007, pp. 1–8. doi:
10.1109/PES.2007.386289.

[28] J. A. Paradiso and T. Starner, “Energy scavenging for mobile and wireless electronics,” *IEEE Pervasive Computing*, vol. 4, no. 1, pp. 18–27, Jan. 2005, doi:
10.1109/MPRV.2005.9.

[29] L.-G. Tran, H.-K. Cha, and W.-T. Park, “RF power harvesting: a review on designing methodologies and applications,” *Micro and Nano Systems Letters*, vol. 5, Dec. 2017, doi: 10.1186/s40486-017-0051-0.

[30] “Energy Harvesting Techniques for Monitoring Devices in Smart Grid Application | IEEE Conference Publication | IEEE Xplore.” Accessed: Mar. 26, 2024.
[Online]. Available: <https://ieeexplore.ieee.org/document/9339526>

[31] S. Kim *et al.*, “Ambient RF Energy-Harvesting Technologies for Self-Sustainable Standalone Wireless Sensor Platforms,” *Proceedings of the IEEE*, vol. 102, no. 11, pp. 1649–1666, Nov. 2014, doi: 10.1109/JPROC.2014.2357031.

- [32] K. T. Thong, B. C. Kok, C. Uttraphan, S. Gareh, and Z. J. Sam, “Data acquisition system for Piezoelectric Cymbal Transducer energy harvesting,” in *2016 IEEE International Conference on Power and Energy (PECon)*, Nov. 2016, pp. 707–711. doi: 10.1109/PECON.2016.7951651.
- [33] H. Nishimoto, Y. Kawahara, and T. Asami, “Prototype implementation of ambient RF energy harvesting wireless sensor networks,” in *2010 IEEE SENSORS*, Nov. 2010, pp. 1282–1287. doi: 10.1109/ICSENS.2010.5690588.
- [34] J. Zhang, Z. P. Wu, C. G. Liu, B. H. Zhang, and B. Zhang, “A double-sided rectenna design for RF energy harvesting,” in *2015 IEEE International Wireless Symposium (IWS 2015)*, Mar. 2015, pp. 1–4. doi: 10.1109/IEEE-IWS.2015.7164617.
- [35] H. Takhedmit, “Ambient RF power harvesting: Application to remote supply of a batteryless temperature sensor,” in *2016 IEEE International Smart Cities Conference (ISC2)*, Sep. 2016, pp. 1–4. doi: 10.1109/ISC2.2016.7580800.
- [36] J. Cheang, W. Cheng, D. Gavrilov, B. Schiller, V. Smagin, and M. Gouzman, “High efficiency powering system for wireless sensor for AC monitoring in smart grid applications,” in *2014 11th International Conference & Expo on Emerging Technologies for a Smarter World (CEWIT)*, Oct. 2014, pp. 1–5. doi: 10.1109/CEWIT.2014.7021142.
- [37] T. Ishiyama, “Indoor Photovoltaic Energy Harvesting and Power Management for IoT Devices,” in *2022 11th International Conference on Renewable Energy Research and Application (ICRERA)*, Sep. 2022, pp. 461–464. doi: 10.1109/ICRERA55966.2022.9922863.

- [38] A. Berger, L. B. Hörmann, C. Leitner, S. B. Oswald, P. Priller, and A. Springer, “Sustainable energy harvesting for robust wireless sensor networks in industrial applications,” in *2015 IEEE Sensors Applications Symposium (SAS)*, Apr. 2015, pp. 1–6. doi: 10.1109/SAS.2015.7133585.
- [39] A. Yoza, K. Uchida, A. Yona, and T. Senjyu, “Optimal operation of controllable loads in DC smart house with EV,” in *2012 International Conference on Renewable Energy Research and Applications (ICRERA)*, Nov. 2012, pp. 1–6. doi: 10.1109/ICRERA.2012.6477315.
- [40] H. Yamauchi, M. Miyagi, K. Uchida, A. Yona, and T. Senjyu, “Advanced Smart House with an electric vehicle,” in *2012 International Conference on Renewable Energy Research and Applications (ICRERA)*, Nov. 2012, pp. 1–6. doi: 10.1109/ICRERA.2012.6477343.
- [41] D. Vadhel, S. Modhavadiya, and J. Zala, “ENERGY GENERATION FROM PELTIER MODULE BY UTILIZING HEAT,” vol. 04, no. 03.
- [42] E. Ouserigha and A. Benjamin, “Evaluation of the Performance of the SP 1848-27145 Thermoelectric Generator Module,” *International Journal of Scientific and Research Publications (IJSRP)*, vol. 12, p. 339, Feb. 2022, doi: 10.29322/IJSRP.12.02.2022.p12246.
- [43] P. Abadi, D. Darlis, and M. Suraatmadja, “Green energy harvesting from human footsteps,” *MATEC Web of Conferences*, vol. 197, p. 11015, Jan. 2018, doi: 10.1051/mateconf/201819711015.

- [44] T. Ruan, Z. J. Chew, and M. Zhu, “Energy-Aware Approaches for Energy Harvesting Powered Wireless Sensor Nodes,” *IEEE Sensors Journal*, vol. 17, no. 7, pp. 2165–2173, Apr. 2017, doi: 10.1109/JSEN.2017.2665680.
- [45] H. Heidarifar and M. Shahbakhti, “Energy saving in a residential building using occupancy information,” in *Progress in Canadian Mechanical Engineering. Volume 6*, Sherbrooke, Canada: Université de Sherbrooke. Faculté de génie, 2023. doi: 10.17118/11143/20840.
- [46] B. Levine, “Interview with Ben Levine from ME Engineers.”
- [47] H. Code, “Interveiw with Hartin Code from Brainbox AI.”
- [48] J. Kelchner, “Interview with John Kelchner from Citizen’s Electric.”
- [49] N. Johnson, “Interview with Nate Johnson from Citizen’s Electric.”
- [50] I. Chaour, A. Fakhfakh, and O. Kanoun, “Enhanced Passive RF-DC Converter Circuit Efficiency for Low RF Energy Harvesting,” *Sensors*, vol. 17, no. 3, Art. no. 3, Mar. 2017, doi: 10.3390/s17030546.
- [51] X. Lu, P. Wang, D. Niyato, D. I. Kim, and Z. Han, “Wireless Networks With RF Energy Harvesting: A Contemporary Survey,” *IEEE Communications Surveys & Tutorials*, vol. 17, no. 2, pp. 757–789, 2015, doi: 10.1109/COMST.2014.2368999.
- [52] “stm8l001j3.pdf.” Accessed: Mar. 09, 2024. [Online]. Available: <https://www.st.com/resource/en/datasheet/stm8l001j3.pdf>

- [53] N. Williams, J. Power, D. Trimble, and S. O'Shaughnessy, "An experimental evaluation of thermoelectric generator performance under cyclic heating regimes," *Heat and Mass Transfer*, Sep. 2022, doi: 10.1007/s00231-022-03280-5.
- [54] C. A. Reynaud, R. Clerc, P. B. Lechêne, M. Hébert, A. Cazier, and A. C. Arias, "Evaluation of indoor photovoltaic power production under directional and diffuse lighting conditions," *Solar Energy Materials and Solar Cells*, vol. 200, p. 110010, Sep. 2019, doi: 10.1016/j.solmat.2019.110010.
- [55] "LTC3108.pdf." Accessed: Mar. 28, 2024. [Online]. Available: <https://www.analog.com/media/en/technical-documentation/data-sheets/LTC3108.pdf>
- [56] "msp430g2553.pdf." Accessed: Mar. 09, 2024. [Online]. Available: <https://www.ti.com/lit/ds/symlink/msp430g2553.pdf>
- [57] "40001607D.pdf." Accessed: Mar. 09, 2024. [Online]. Available: <https://www1.microchip.com/downloads/aemDocuments/documents/OTH/ProductDocuments/DataSheets/40001607D.pdf>
- [58] "stm81050j3.pdf." Accessed: Mar. 09, 2024. [Online]. Available: <https://www.st.com/resource/en/datasheet/stm81050j3.pdf>
- [59] S. Shanmugam, V. Selvaraj, R. Kasirajan, H. Sivakumar, and K. Kandasamy, "Household Energy Conservation Using Piezoelectric Tiles and solar Tracker," *IOP Conf. Ser.: Mater. Sci. Eng.*, vol. 955, no. 1, p. 012071, Nov. 2020, doi: 10.1088/1757-899X/955/1/012071.
- [60] "XBee/XBee-PRO S1 802.15.4 (Legacy) User Guide".

[61] V. Pop *et al.*, “Wireless autonomous sensor technology for body area networks,”
in *16th Asia and South Pacific Design Automation Conference (ASP-DAC 2011)*,
Yokohama, Japan: IEEE, Jan. 2011, pp. 561–566. doi: 10.1109/ASPDAC.2011.5722253.